optical and confocal microscope images taken on block copolymer coated surfaces. A large number of cells adhered to and proliferated on the noncoated TCPS surface, because of the large amount of cell-adhesive serum proteins on the TCPS surface. On the other hand, only a limited number of cells were observed on the PM1 surface, which consisted of maximum PMPC monomer composition. Moreover, most of the observed cells were nonadhesive; i.e., they maintained a globular form thought of as a nonbiospecific physical adhesion. The number of adhered cells on the block copolymer surface increased as the number of PDMS monomer composition increased (from PM1 to PM3). Because the PDMS domain ratio increased as the PDMS monomer composition increased, this phenomenon is thought to occur because of the increased adsorption of serum proteins on hydrophobic PDMS domains.

Cell adhesion behavior on PM3 has a significant meaning in this work. Usually MPC polymer-containing materials exhibit an antibiofouling nature because of the thick hydrated layer that forms around the phosphorylcholine group [13]. As a result, homogeneously prepared MPC polymer surfaces normally have low water contact angles (0–20°), and they do not display a cell-adhesive surface nature, even though their MPC monomer composition is only around 30% [28]. For that reason, biocompatibility of MPC polymer-containing biomaterials has normally been determined by studying the hydrophilicity of the surfaces with a monomer composition of MPC. However, in our current study, we have been able to confirm that a heterogeneously prepared hydrophilic polymer surface (i.e., one with a water contact angle of less than 20°) induced a large number of cells to

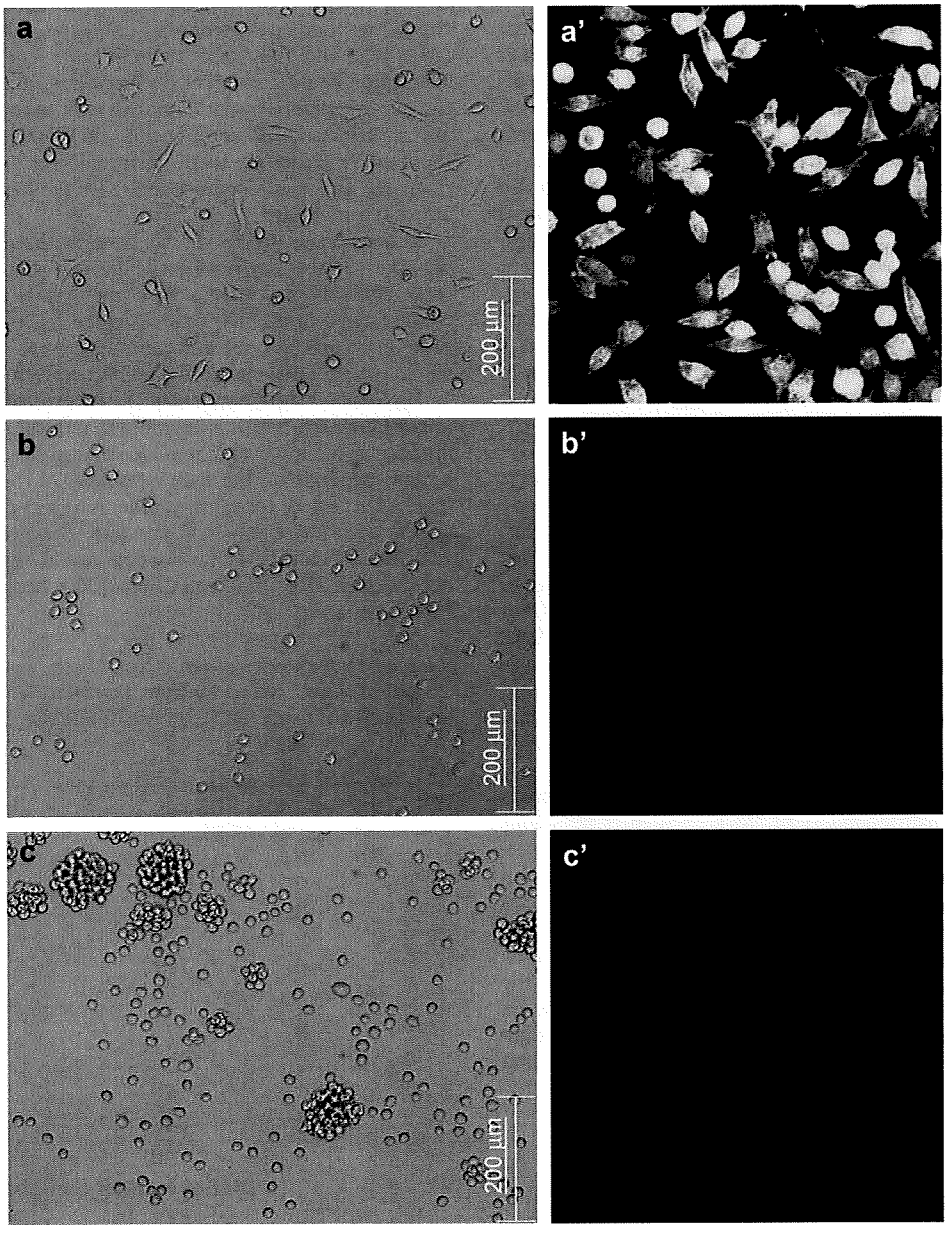

Fig. 10. Optical and confocal microscope images of block copolymer surfaces taken after two days of cultivation in serum-free medium. (a), (a') noncoated TCPS; (b), (b') PM1; (c), (c') PM2; (d), (d') PM3; and (e), (e') PDMS. Scale bar in optical image = 200 μm. Scan size of confocal images = 300 μm × 300 μm.

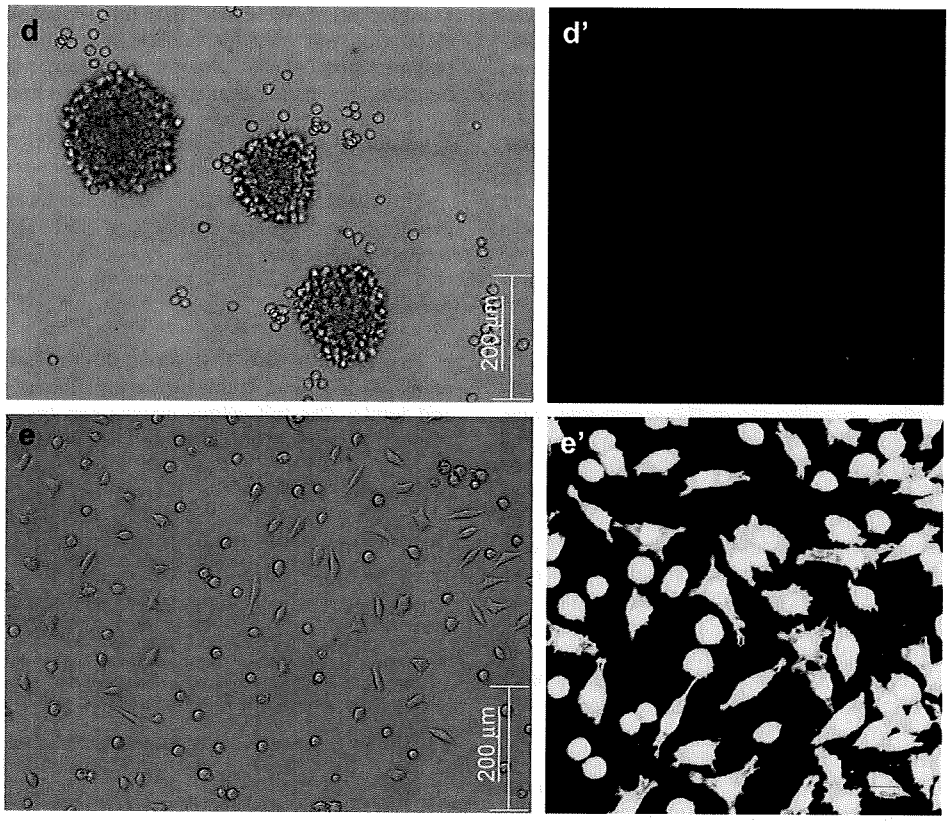

Fig. 10. (*continued*).

adhere onto its surface even though the MPC monomer composition was around 45% (PM3). This result emphasizes the importance of surface morphologies in designing a biomaterial. In other words, heterogeneously segregated hydrophobic domains can have a significant effect on cellular response, even with a hydrophilic MPC polymer surface. Cell proliferation on block copolymer templates at a 10% FBS level is summarized in Fig. 9.

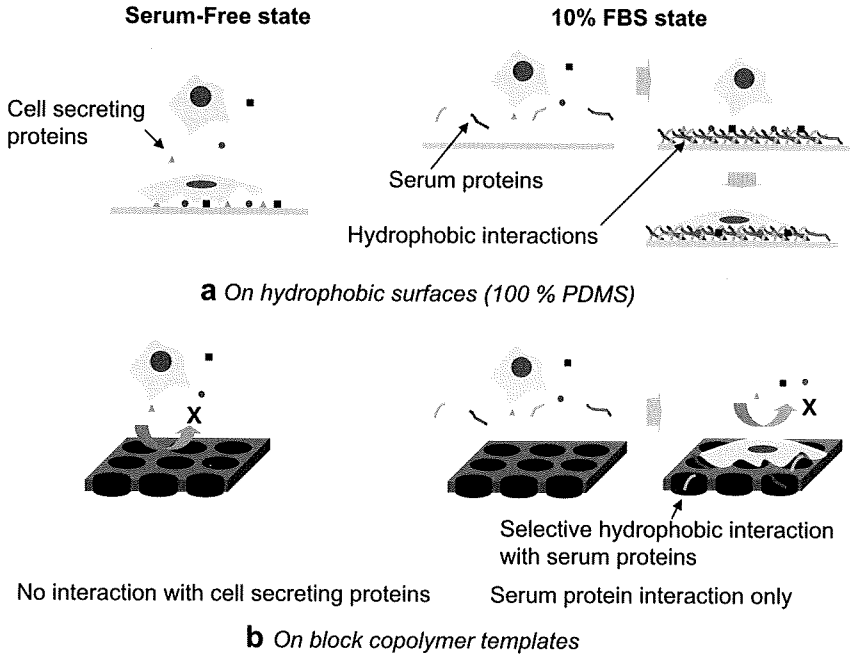

Scheme 2. Schematic explanations of serum protein-block copolymer interaction and resulting cell adhesion behavior.

In order to investigate the effect of serum proteins on cell adhesion behavior, a cell adhesion test was carried out in a serum-free medium. As shown in Fig. 8, no significant cell proliferation was observed on any of the sample surfaces in serum-free medium, including the PDMS/noncoated TCPS control surfaces due to the lack of growth factors and cell adhesive serum proteins. However, cellular responses observed for PDMS/noncoated TCPS and block copolymer surfaces were clearly different.

Fig. 10 presents optical and confocal microscopy images of cells on sample surfaces in a serum-free medium. Although cells were not proliferated, strong cell attachments were observed on hydrophobic TCPS and PDMS surfaces. On the other hand, no cells adhered on any of the block copolymer surfaces. Cell adhesion on materials surfaces, especially for fibroblasts, is controlled mainly by the extracellular matrix (ECM), which is induced by plasma proteins and cell-secreting proteins [32]. In the serum-free state, a serum-induced ECM could not be generated to bring about cell adhesion; therefore, only cell-secreting proteins could affect cell adhesion behavior. On 100% hydrophobic surfaces such as TCPS or PDMS, these secreted proteins seemed to have an effect on cell adhesion behavior that was probably caused by strong hydrophobic interactions between the proteins and the surfaces. However, heterogeneously prepared MPC polymer surfaces suppressed the effect of these secreted proteins.

There are two possible explanations for this result. One possibility is the density problem of cell-adhesive proteins on block copolymer surfaces. Because hydrophobic domains exist only sparsely on the PMPC matrix, the adsorbed cell adhesion factors, "without serum proteins," may not be sufficient to induce cell adhesion. Of course, this hypothesis would have to be demonstrated with much more experimental evidence, such as quantitative analysis of surface-adsorbed proteins, and exact adsorption distribution of serum proteins on heterogeneous surfaces, which is out of the range of this current study. Another possible explanation is the size effect of cell-adhesive proteins and segregated PDMS domains. Fig. 7 makes clear that the overall amount of adsorbed proteins decreases as the molecular weight of the protein increases (e.g., IgG ~ 150 kDa, Fibronectin ~ 440 kDa). Because the hydrophobic PDMS domain exists only to a limited extent on PMPC domains with a nanoscale size, protein molecules with higher molecular weight might have a rare chance to adsorb onto it, as previously reported (size effect) [33]. Cell adhesion factors including laminin, secreted by the fibroblast itself, have a much higher molecular weight (~900 kDa) compared to other cell-adhesive proteins contained in serum. As a result, we speculate that this size effect could be a cause of the noncellular adhesive nature of the block copolymer surface in a serum-free condition, as shown in Scheme 2.

Further investigation of protein distribution on block copolymer surfaces is now underway. In any event, we wish to emphasize that segregated hydrophobic domains on MPC polymer surfaces have a significant effect on cellular response under serum conditions.

4. Conclusions

We investigated protein adsorption and cell adhesion behavior on heterogeneously prepared MPC polymer surfaces. Although MPC polymers are well known to be noncell adhesive, and, thus, do not promote cell proliferation, existing heterogeneous hydrophobic PDMS domains strongly affect serum protein adsorption and cell adhesion behavior. From our investigation, we conclude that segregated hydrophobic domains have to be taken into account when designing serum contact biomaterials that contain MPC polymers, even though the surface reveals a higher level of hydrophilicity, owing to the large amount of phosphorylcholine groups present. We expect that this suggestion could be a useful inspiration not only for understanding of cellular response on polymer surfaces, but also for designing cell attachable various biomaterial surfaces applied in cell and tissue engineering.

Acknowledgement

This research was partially supported by the Core Research for Evolution Science and Technology (CREST), Japan Science and Technology Agency.

Appendix

Figures with essential colour discrimination. Scheme 2 and many of the figures in this article are difficult to interpret in black and white. The full colour images can be found in the on-line version, at doi:10.1016/j.biomaterials.2009.06.031.

References

[1] Horbett TA, Brash JL. Proteins at interfaces II: fundamentals and applications. In: ACS symposium series, vol. 602. Washington, DC: American Chemical Society; 1995. p. 2–14.
[2] Shen MC, Wagner MS, Castner DG, Ratner BD, Horbett TA. Multivariate surface analysis of plasma-deposited tetraglyme for reduction of protein adsorption and monocyte adhesion. Langmuir 2003;19:1692–9.
[3] Kwak D, Wu Y, Horbett TA. Fibrinogen and von Willebrand's factor adsorption are both required for platelet adhesion from sheared suspensions to polyethylene preadsorbed with blood plasma. J Biomed Mater Res A 2005;74:69–82.
[4] Sousa A, Sengonul M, Latour R, Kohn J, Libera M. Selective protein adsorption on a phase separated solvent-cast polymer blend. Langmuir 2006;22:6286–92.
[5] Kohr HL, Kuan Y, Kukula H, Tamada K, Knoll W, Moeller M, et al. Response of cells on surface-induced nanopatterns: fibroblasts and mesenchymal progenitor cells. Biomacromolecules 2007;8:1530–40.
[6] Arnold M, Hirschfeld WVC, Lohmuller T, Heil P, Blummel J, Cavalcanti AEA, et al. Induction of cell polarization and migration by a gradient of nanoscale variations in adhesive ligand spacing. Nano Lett 2008;8:2063–9.
[7] Iwasaki Y, Yamasaki A, Ishihara K. Platelet compatible blood filtration fabrics using a phosphorylcholine polymer having high surface mobility. Biomaterials 2003;24:3599–604.
[8] Ishihara K, Ziats NP, Tierney BP, Nakabayashi N, Anderson JM. Protein adsorption from human plasma is reduced on phospholipids polymers. J Biomed Mater Res 1991;25:1397–407.
[9] Ishihara K, Aragaki R, Ueda T, Watanabe A, Nakabayashi N. Reduced thrombogenicity of polymers having phospholipids polar groups. J Biomed Mater Res 1990;24:1069–77.
[10] Lewis AL, Hughes PD, Kirkwood LC, Leppard SW, Redman RP, Tolhurst LA, et al. Synthesis and characterization of phosphorylcholine-based polymers useful for coating blood filtration devices. Biomaterials 2000;20:1847–59.
[11] Kimura M, Takai M, Ishihara K. Tissue-compatible and adhesive polyion complex hydrogels composed of amphiphilic phospholipid polymers. J Biomater Sci Polym Ed 2007;18:623–40.
[12] Ye SH, Watanabe J, Iwasaki Y, Ishihara K. In situ modification on cellulose acetate hollow fiber membrane modified with phospholipid polymer for biomedical application. J Membr Sci 2005;249:133–41.
[13] Ishihara K, Nomura H, Mihara T, Kurita K, Iwasaki Y, Nakabayashi N. Why do phospholipid polymers reduce protein adsorption? J Biomed Mater Res 1998;39:323–30.
[14] Konno T, Ishihara K. Temporal and spatial controllable cell encapsulation hydrogel composed of a novel water-soluble phospholipid polymer containing phenylboronic acid. Biomaterials 2007;28:1770–7.
[15] Ueda T, Oshida H, Kurita K, Ishihara K, Nakabayashi N. Preparation of 2-methacryloyloxyethyl phosphorylcholine copolymers with alkyl methacrylates and their blood compatibility. Polym J 1992;24:1259–69.
[16] Moro T, Takatori Y, Ishihara K, Konno T, Takigawa Y, Matsushita T, et al. Surface grafting of artificial joints with a biocompatible polymer for preventing periprosthetic osteolysis. Nat Mater 2004;3:829–36.
[17] Jang KH, Sato K, Konno T, Ishihara K, Kitamori T. Modification by 2-methacrylolyoxyethyl phosphorylcholine coupled to a photolabile linker for cell micropatterning. Biomaterials 2009;30:1413–20.
[18] Yamane T, Maruyama O, Nishida M, Kosaka R, Chida T, Kawamura H, et al. Antithrombogenic properties of a monopivot magnetic suspension centrifugal pump for circulatory assist. Artif Organs 2008;32:484–9.
[19] Morimoto N, Iwasaki Y, Nakabayashi N, Ishihara K. Physical properties and blood compatibility of surface modified segmented polyurethane by semi-interpenetrating polymer networks with a phospholipid polymer. Biomaterials 2002;24:4881–7.

[20] Ishihara K, Fukumoto K, Iwasaki Y, Nakabayashi N. Modification of polysulfone with phospholipid polymer for improvement of the blood compatibility. Part 2. Protein adsorption and platelet adhesion. Biomaterials 1999;20:1553–9.
[21] Ishihara K, Fujita H, Yoneyama T, Iwasaki Y. Antithrombogenic polymer alloy composed of 2-methacryloyloxyethyl phosphorylcholine polymer and segmented polyurethane. J Biomater Sci Polym Ed 2000;11:1183–95.
[22] Morimoto N, Iwasaki Y, Nakabayashi N, Ishihara K. Physical properties and blood compatibility of surface modified segmented polyurethane by semi-interpenetrating polymer networks with a phospholipid polymer. Biomaterials 2002;23:4881–7.
[23] Kim HI, Takai M, Ishihara K. Bioabsorbable material-containing phosphorylcholine group-rich surfaces for temporary scaffolding of the vessel wall. Tissue Eng Part A 10.1089/ten.tea.2008.0307
[24] Fasolka MJ, Mayes AM. Block copolymer thin films: physics and applications. Annu Rev Mater Res 2001;31:323–55.
[25] Ishihara K, Ueda T, Nakabayashi N. Preparation of phospholipid polymers and their properties as polymer hydrogel membrane. Polym J 1990;22:355–60.
[26] Seo JH, Matsuno R, Konno T, Takai M, Ishihara K. Surface tethering of phosphorylcholine groups onto poly(dimethylsiloxane) through swelling-deswelling methods with phospholipids moiety containing ABA-type block copolymers. Biomaterials 2008;29:1367–76.
[27] Cooke DM, Shi AC. Effects of polydispersity on phase behavior of diblock copolymers. Macromolecules 2006;39:6661–71.
[28] Futamura K, Matsuno R, Konno T, Takai M, Ishihara K. Rapid development of hydrophilicity and protein adsorption resistance by polymer surfaces bearing phosphorylcholine and naphthalene groups. Langmuir 2008;24:10340–4.
[29] Okano T, Aoyagi T, Kataoka K, Abe K, Sakurai Y. Hydrophilic–hydrophobic microdomain surfaces having an ability to suppress platelet aggregation and their in vitro antithrombogenicity. J Biomed Mater Res 1998;20:919–28.
[30] Kumar N, Parajuli O, Gupta A, Hahm JI. Elucidation of protein adsorption behavior on polymeric surfaces: toward high-density, high-payload protein templates. Langmuir 2008;24:2688–94.
[31] Kumar N, Hahm JI. Nanoscale protein patterning using self-assembled diblock copolymers. Langmuir 2005;21:6652–5.
[32] Nolte SV, Xu W, Rennekampff HO, Rodemann HP. Diversity of fibroblasts – a review on implications for skin tissue engineering. Cells Tissues Organs 2008;187:165–76.
[33] Lazos D, Franzka S, Ulbricht M. Size-selective protein adsorption to polystyrene surfaces by self-assembled grafted poly(ethylene glycols) with varied chain lengths. Langmuir 2005;21:8774–84.

Colloids and Surfaces B: Biointerfaces 74 (2009) 96–102

Contents lists available at ScienceDirect

Colloids and Surfaces B: Biointerfaces

journal homepage: www.elsevier.com/locate/colsurfb

Surface modification of a titanium alloy with a phospholipid polymer prepared by a plasma-induced grafting technique to improve surface thromboresistance

Sang Ho Ye[a,b], Carl A. Johnson Jr[a,c], Joshua R. Woolley[a,c], Heung-Il Oh[a,d], Lara J. Gamble[e], Kazuhiko Ishihara[f], William R. Wagner[a,b,c,d,*]

[a] McGowan Institute for Regenerative Medicine, University of Pittsburgh, 100 Technology Dr., Suite 200, Pittsburgh, PA 15219, USA
[b] Department of Surgery, University of Pittsburgh, Pittsburgh, PA 15219, USA
[c] Department of Bioengineering, University of Pittsburgh, Pittsburgh, PA 15219, USA
[d] Department of Chemical Engineering, University of Pittsburgh, Pittsburgh, PA 15219, USA
[e] Departments of Bioengineering and NESAC/BIO, University of Washington, Seattle, WA 98195, USA
[f] Department of Materials Engineering, School of Engineering, The University of Tokyo, 7-3-1, Hongo, Bunkyo-ku, Tokyo 113-8656, Japan

ARTICLE INFO

Article history:
Received 10 April 2009
Received in revised form 26 June 2009
Accepted 29 June 2009
Available online 7 July 2009

Keywords:
Titanium alloy
Surface modification
Phospholipid polymer
Blood compatibility
Ventricular assist device (VAD)

ABSTRACT

To improve the thromboresistance of a titanium alloy ($TiAl_6V_4$) surface which is currently utilized in several ventricular assist devices (VADs), a plasma-induced graft polymerization of 2-methacryloyloxyethyl phosphorylcholine (MPC) was carried out and poly(MPC) (PMPC) chains were covalently attached onto a $TiAl_6V_4$ surface by a plasma induced technique. Cleaned $TiAl_6V_4$ surfaces were pretreated with H_2O-vapor-plasma and silanated with 3-methacryloylpropyltrimethoxysilane (MPS). Next, a plasma-induced graft polymerization with MPC was performed after the surfaces were pretreated with Ar plasma. Surface compositions were verified by X-ray photoelectron spectroscopy (XPS). In vitro blood biocompatibility was evaluated by contacting the modified surfaces with ovine blood under continuous mixing. Bulk phase platelet activation was quantified by flow cytometric analysis, and surfaces were observed with scanning electron microscopy after blood contact. XPS data demonstrated successful modification of the $TiAl_6V_4$ surfaces with PMPC as evidenced by increased N and P on modified surfaces. Platelet deposition was markedly reduced on the PMPC grafted surfaces and platelet activation in blood that contacted the PMPC-grafted samples was significantly reduced relative to the unmodified $TiAl_6V_4$ and polystyrene control surfaces. Durability studies under continuously mixed water suggested no change in surface modification over a 1-month period. This modification strategy shows promise for further investigation as a means to reduce the thromboembolic risk associated with the metallic blood-contacting surfaces of VADs and other cardiovascular devices under development.

1. Introduction

Suboptimal blood compatibility in many cardiovascular devices puts patients at increased risk for thromboembolism, often necessitating the use of chronic anti-coagulation and its accompanying increased risk for bleeding. The composition of the biomaterial surface, the nature of the blood flowing across the device surfaces and the bias of the patient's blood toward hemostatic reactions all combine to define thrombotic and thromboembolic risk. Thus much work has focused on utilizing computational fluid dynamics to improve flow characteristics over biomaterial surfaces in circulatory support devices [1] and similarly there has been great interest in developing chemical modifications for blood contacting surfaces [2].

Our recent interest has been in developing a rotary blood pump for pediatric applications in which aggressive anticoagulation may be problematic and biocompatibility is thus of primary concern. For design and machinability considerations the titanium alloy $TiAl_6V_4$ makes up the blood contacting surfaces of this pump as well as several other rotary blood pumps in clinical use and in pre-clinical development [1,3–9]. Although titanium and its alloys have exhibited generally acceptable biocompatibility in a variety of settings, its surface modification remains of interest for blood contact since platelet deposition still can occur in vitro and thrombosis and thromboembolism can occur in these devices in vivo [10–12].

Biomaterial surface modification by plasma based techniques has frequently been applied due to the high efficiency of this

* Corresponding author at: McGowan Institute for Regenerative Medicine, University of Pittsburgh, 100 Technology Dr., Suite 200, Pittsburgh, PA 15219, USA. Tel.: +1 412 512 5110.
E-mail address: wagnerwr@upmc.edu (W.R. Wagner).

0927-7765/$ – see front matter © 2009 Elsevier B.V. All rights reserved.
doi:10.1016/j.colsurfb.2009.06.032

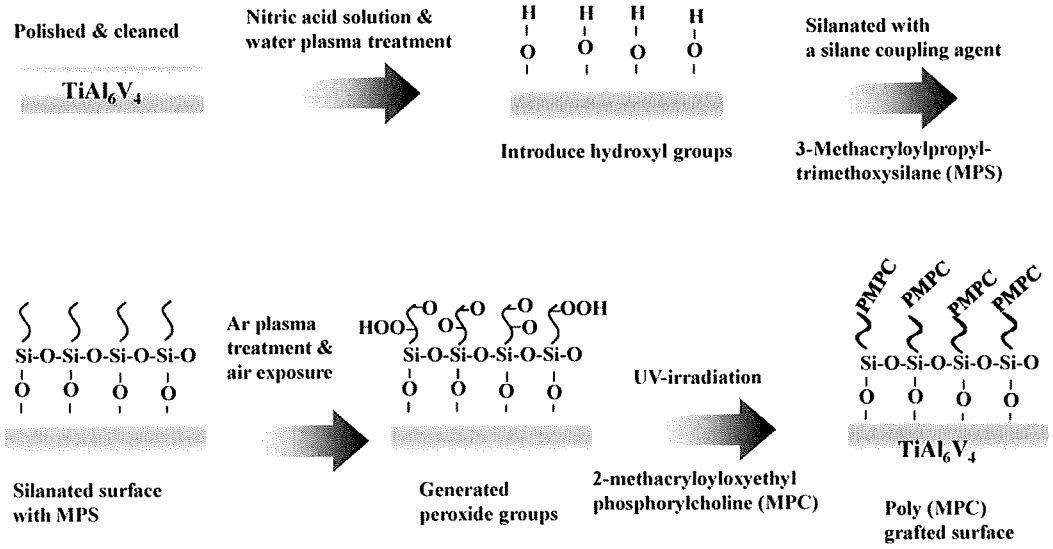

Fig. 1. Scheme of surface functionalization and modification of a $TiAl_6V_4$ surface with PMPC.

approach for a variety of substrates and geometry [13]. Active functional groups can be introduced by utilizing a specific atmosphere such as water, ammonia or argon (Ar) which allows further modification by covalent attachment of other polymers or biomolecules on the substrate [14–17]. Plasma induced graft polymerization after Ar plasma pretreatment is attractive for its high efficiency and others have previously reported on the effects of plasma treatment time, plasma power and storage time on surface modifications with this method [18,19]. Polytetrafluoroethylene, silicon, and stainless steel surfaces have successfully been modified by Ar plasma induced grafting copolymerization with a poly (ethylene glycol) containing macromonomer to improve their surface blood compatibility [20–22].

Synthetic phospholipid polymers (phosphorylcholine (PC) group-bearing polymers) have been extensively studied due to their excellent biological and blood compatibility [23]. One of the most representative phospholipid polymers, 2-methacryloyloxyethylphosphorylcholine (MPC) polymer has received considerable interest for medical applications [24–26]. Many researchers have shown previously that surface modification with the MPC polymers or the introduction of PC groups by blending, coating and graft modification techniques are effective in improving blood compatibility by resisting non-specific protein adsorption and platelet activation and adhesion on polymer biomaterial surfaces [27–31]. The MPC polymers have also been applied to some metallic biomaterial surfaces including ventricular assist devices (VADs) and demonstrated apparent improvements in blood compatibility [32–35]. However, to date most of the surface modification techniques with the MPC polymers involve physical adsorption onto metallic surfaces. We recently reported on the MPC polymer covalent immobilization approach for $TiAl_6V_4$ that showed promise in improving blood biocompatibility [36]. While effective, concerns with this technique were the lability of the amide bond linking the copolymer to the surface and the extent of surface coverage that might be achieved.

Our objective in this study was to introduce a new, potentially more robust method of polymerizing MPC off of a modified $TiAl_6V_4$ surface using a plasma-induced graft technique that might offer durability under high shear and for extended blood contacting periods. The modified $TiAl_6V_4$ surface was characterized in terms of its surface composition and acute platelet deposition and activation after contact with ovine blood in vitro.

2. Materials and methods

2.1. Materials

A titanium alloy ($TiAl_6V_4$) sheet was obtained from California Metal & Supply Inc., Gardena, CA. MPC was obtained from NOF Corp. (Tokyo, Japan), which was synthesized as previously described [24]. 3-Methacryloylpropyltrimethoxysilane (MPS, Aldrich, USA) was used as a silane coupling agent. Heparin (Pharmacia & Upjohn Co., Ann Arbor, MI) was used for blood anticoagulation.

2.2. Surface pretreatment and silanization of a $TiAl_6V_4$

The $TiAl_6V_4$ sheet was polished with 3.0, 1.0, 0.25, and 0.1 μ diamond pastes in sequence (Electron Microscopy Sciences, Washington, PA) and cleaned ultrasonically three times for 5 min each with ethanol and acetone. The surfaces were then passivated with a 35% nitric acid solution for 1 h and rinsed with distilled water. Next, the $TiAl_6V_4$ surfaces were pretreated under H_2O plasma with radio frequency glow discharge (RFGD, MARCH GCM250, March Instrument Inc, CA). The RFGD power applied was 25 W at a frequency of 13.65 MHz. The titanium surface was subjected to RFGD for 5 min supplying H_2O vapor at a vacuum pressure of 0.4 Torr. The H_2O plasma pre-treated $TiAl_6V_4$ surfaces were silanated by immersion in an MPS solution for 3 h in a 90 °C oil bath. The MPS solution consisted of 2% MPS in ethanol that was hydrolyzed by adding water and stirring for 1 h. The pH of the MPS solution was adjusted to approximately 3–4 by adding 0.1 M HCl. The silanated samples were dried at 110 °C for 1 h, then rinsed repeatedly with ethanol and water, and stirred in deionized water for 1 h to remove adsorbed MPS. Samples treated in this manner were referred to as Ti-MPS (Fig. 1).

2.3. Plasma-induced surface graft modification with MPC

The silanated $TiAl_6V_4$ samples were treated with Ar plasma by using RFGD (25 W, 20 s, 0.6 Torr), and then the surface was exposed to the atmosphere for 10 min to create surface peroxide groups. The $TiAl_6V_4$ sample was then immersed in MPC solution (0.5 mM) which was placed in a transparent polystyrene round-bottom tube (BD Bioscience, San Jose, CA) The monomer solution was passed through argon gas for 1 min and 0.005 mM

riboflavin (Sigma–Aldrich, St. Louis, MO) was added to eliminate any oxygen [14]. Then, graft modification onto the $TiAl_6V_4$ surface was carried out under a high intensity UV lamp for 24 h. This decomposed the surface peroxide groups to free radicals and poly(MPC) (PMPC) was grafted from the surface. The modified samples were rinsed three times with ethanol and water and stirred in deionized water for 24 h to remove physically adsorbed PMPC. Samples treated in this manner were referred to as Ti–MPS–PMPC (Fig. 1).

2.4. Surface characterization

The surface composition of the titanium samples was analyzed by X-ray photoelectron spectroscopy (XPS) using a surface science instruments S-probe spectrometer and a take-off angle of photoelectron was 55°. The Service Physics ESCAVB Graphics Viewer program was used to determine peak area, calculate the elemental compositions from peak areas, and peak fit the high-resolution spectra. The surface composition on a given sample was averaged from three composition spots for each sample. The mean value for three different samples was determined.

The static contact angle of water on the surfaces of unmodified and modified titanium samples was measured at room temperature using a contact angle goniometer (VCA optima, AST Product Inc., Billerica, MA) by placing 1 μL of double distilled water on the surfaces. The droplet was imaged using a video camera coupled to a light microscope, and the contact angle was determined on the screen of a monitor employing imaging software. Five measurements were made on each sample to obtain the contact angle of the sample. The contact angle was also measured weekly in several of the modified samples that underwent continuous stirring under deionized water for 1 month to test the long term stability of the surface modification. XPS was also performed on the surfaces after 1 month of water contact.

2.5. Blood collection and blood contact test

Whole ovine blood was collected by jugular venipuncture directly into a syringe containing heparin (3.0 or 6.0 U/mL for 1 and 2.5 h blood contacting experiments, respectively) using an 18 gauge 1 ½″ needle, after discarding the first 3 mL. NIH guidelines for the care and use of laboratory animals were observed. Modified titanium and unmodified samples were placed into Vacutainer® blood collection tubes without additives (BD Biosciences, Franklin Lakes, NJ) filled with heparinized ovine blood and incubated for a specified time at 37 °C on a hematology mixer (Fisher Scientific, Pittsburgh, PA).

2.6. Observation and quantification of platelet deposition and activation

The $TiAl_6V_4$ surfaces were observed by scanning electron microscopy (SEM; JSM-6330F, JEOL USA, Inc., Peabody, MA) after 2.5 h contact with heparinized blood (6.0 U/mL). The $TiAl_6V_4$ surfaces were also observed with epi-fluorescence microscopy (ZEISS, Carl Zeiss, Inc. Thornwood, NY) after contact for 1 h with heparinized blood (3.0 U/mL) that was treated with quinacrine dihydrochloride (10 μM final concentration, Sigma) to fluorescently label the platelets. The number of platelets for each sample was also estimated by a lactate dehydrogenase (LDH) assay [37] with an LDH Cytotoxicity Detection Kit (Clonetech Laboratories Inc., CA). In this assay, the surfaces were rinsed thoroughly with 50 mL PBS following 2.5 h contact with blood (6.0 U/mL heparin) and then immersed in 1 mL of 2% Triton X-100 solution (Sigma) for 20 min to lyse deposited platelets. Calibration of spectrophotometer absorbance results to platelet numbers was accomplished using a calibration curve generated from known dilutions of ovine platelet rich plasma in the lysing solution.

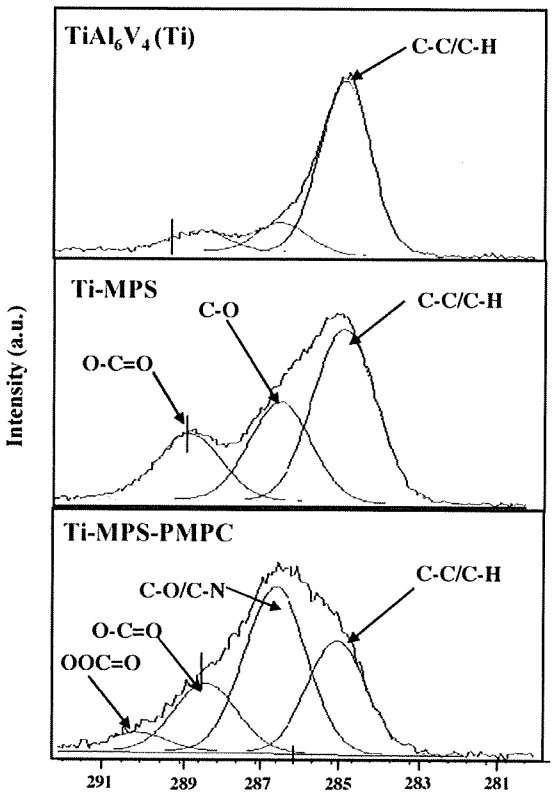

Fig. 2. XPS high resolution (C1s) spectra of the modified and unmodified $TiAl_6V_4$ samples.

The percentage of activated ovine platelets in the bulk phase of the blood during surface contact was determined using flow cytometric quantification of Annexin V binding as recently described [38]. Blood samples (10 μL) were taken during test surface contact experiments described above for LDH measurement of platelet deposition after 2 h. Activation levels from five independent samples were averaged for each surface type.

2.7. Statistical analyses

Data are presented as means with standard deviation. Statistical significance between sample groups was determined using ANOVA followed by post-hoc Newman–Keuls testing and accepted at $p < 0.05$.

3. Results

The high-resolution spectra from XPS are shown in Fig. 2. The C1s data was calibrated to the hydrocarbon peak (C–C/C–H) at 285.0 eV. The MPS modified $TiAl_6V_4$ surface (Ti–MPS) showed an increase in the peak at 286.6 eV and 288.5 eV which is likely due to C–O and O–C=O type species. The PMPC modified $TiAl_6V_4$ surface showed a further increase in the peak at 286.6 eV by the addition of the C–N type species that are attributed to the MPC units. Furthermore, the Ti–MPS–PMPC also has a peak at 290.5 eV which is likely due to peroxide OOC=O type species that is attributed to the Ar plasma treatment. The surface atomic compositions of $TiAl_6V_4$ samples are shown in Table 1. The oxygen composition of the pre-treated $TiAl_6V_4$ surfaces (Ti–H_2O plasma) rose significantly in comparison with the Ti which was not pre-treated ($p < 0.05$). The MPS mod-

Table 1
Atomic percentage by X-ray photoelectron spectroscopy.

	C	O	Ti	Al	Si	N	P
$TiAl_6V_4$ (Ti)	42.0 (±8.0)	41.1 (±5.2)	9.5 (±1.1)	4.3 (±3.1)	1.0 (±1.0)	1.0 (±0.5)	0.1 (±0.2)
Ti (H_2O plasma)	24.1 (±6.6)	50.8 (±0.4)	10.5 (±3.3)	2.3 (±1.1)	1.3 (±1.4)	0.8 (±0.3)	0.0 (±0.0)
Ti–MPS	49.4 (±8.9)	34.3 (±5.4)	1.3 (±1.3)	1.2 (±1.1)	13.9 (±4.8)	0.2 (±0.4)	0.0 (±0.0)
Ti–MPS–PMPC	42.8 (±12.6)	40.0 (±7.8)	1.4 (±1.6)	0.0 (±0.0)	14.1 (±3.8)	1.8 (±0.3)*	1.0 (±0.2)*

$N = 7$, ± standard deviation for Ti. $N = 3$, ± standard deviation for Ti (H_2O plasma). $N = 5$, ± standard deviation for Ti–MPS. $N = 4$, ± standard deviation for Ti–MPS–PMPC.
* $p < 0.05$ vs. other surfaces.

Table 2
Surface tension on the unmodified and modified titanium samples.

	$TiAl_6V_4$ (Ti)	Ti (H_2O plasma)	Ti–MPS	Ti–MPS–PMPC
Contact angle (°)	58.3 (±6.2)	34.7 (±4.4)	87.6 (±6.4)	18.1 (±4.0)*

$n = 3$, ± standard deviation.
* $p < 0.05$ vs. other surfaces.

ified surface showed an increase in Si which was attributed to the presence of MPS ($p < 0.05$). Furthermore, the XPS data from Ti–MPS–PMPC provide evidence for the successful modification with PMPC by reflecting increased nitrogen (N) and phosphorus (P) ($p < 0.05$).

The surface tension on the modified and unmodified titanium samples was shown in Table 2. The contact angle on $TiAl_6V_4$ surfaces was decreased from 58 ± 6° to 35 ± 4° after H_2O plasma treatment. The Ti–MPS increased in surface tension to 88 ± 6° due to modification with hydrophobic MPS on the $TiAl_6V_4$ surface. However, the surface tension of the PMPC grafted surfaces decreased substantially (Ti–MPS–PMPC = 18 ± 4°) by modification with the hydrophilic PMPC on the surface in comparison with all of the other surfaces ($p < 0.05$). The surface contact angle on the PMPC grafted surface (Ti–MPS–PMPC) measured every 7 days during a 1-month period of mixing with water did not significantly change (Fig. 3). Additionally, the surface composition of several of the modified samples was also measured after mixing for 1 month in water. The XPS analysis results also showed no significant difference in the surface composition of phosphorus before (*P*: 1.1 ± 0.1%) and after (*P*: 1.0 ± 0.1%) the water contacting experiment.

The modified and unmodified $TiAl_6V_4$ surfaces after contact with anticoagulated ovine blood for 1 h at 37 °C were observed with an epi-fluorescence microscope (Fig. 4). Fluorescent platelets are seen to be adhered and aggregated on the surface. The unmodified titanium had relatively high numbers of deposited platelets, whereas the PMPC modified surfaces (Ti–MPS–PMPC) showed few adherent platelets. Platelet adhesion and morphology was also observed with SEM after contact with ovine blood for 2.5 h at 37 °C. The SEM images on the surfaces of the positive control polystyrene, unmodified and modified titanium samples are seen in Fig. 5. The polystyrene control surface (Fig. 5A) supported heavy platelet deposition with most of the deposited platelets exhibiting extended pseudopodia. The unmodified titanium surface (Fig. 5B) had a moderate amount of deposited platelets on its surface, with the number of platelets appearing to be less than for the polystyrene surface. The silanated titanium surface (Ti–MPS, Fig. 5C) also showed a moderate amount of deposited platelets, and these platelets exhibited extended pseudopodia. The quantity of adhered platelets on the Ti–MPS surface appeared to be slightly more than for the unmodified titanium (Fig. 5B). Platelet deposition was decreased dramatically on the Ti–MPS–PMPC surfaces, and the platelets that were adhered generally retained their discoid morphology with some pseudopodia extension (Fig. 5D). It is worth noting that it was difficult to identify adhered platelets on the Ti–MPS–PMPC surface. The number of deposited platelets as quantified by the lactate dehydrogenase (LDH) assay after blood contact (Fig. 6) was significantly less for Ti–MPS–PMPC surfaces than for all of the other surfaces ($p < 0.01$). Flow cytometric quantification of bulk phase platelet activation using the Annexin V assay (Fig. 7) was also significantly lower in blood contacting Ti–MPS–PMPC surfaces than for unmodified titanium and polystyrene samples ($p < 0.05$).

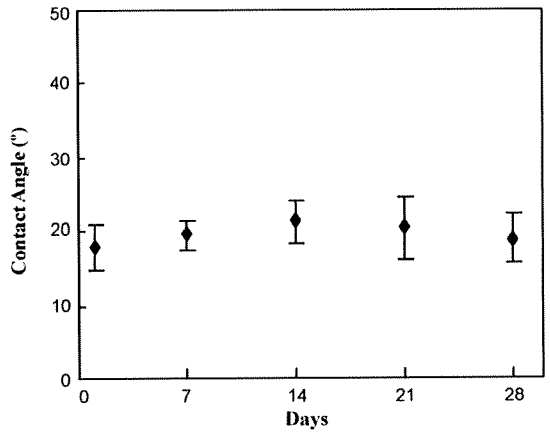

Fig. 3. Contact angle measurements of the PMPC modified $TiAl_6V_4$ surface (Ti–MPS–PMPC) after continuous mixing under deionized water.

4. Discussion

Improvement of surface blood compatibility is of keen interest to the cardiovascular device community given the morbidity and mortality associated with device-related thrombotic complications and with the anticoagulation applied to minimize these risks. In the case of VADs, biocompatibility concerns are a major reason why these devices are underutilized in heart failure patients [3,39–41]. PC groups and PC group-bearing polymer modified surfaces have previously demonstrated marked improvement in blood compatibility when compared to unmodified surfaces [24–31]. Moreover studies involving self-assembled monolayers (SAM) with well defined and highly ordered and oriented PC groups have shown that this type of surface is one of the most promising for anti-fouling since it strongly resists non-specific protein adsorption and cell adhesion [42–44]. There are several successful studies where a PC group-bearing polymer was physically adsorbed onto the metallic surfaces in vascular stent and VAD applications [9,33,34]. In the VAD studies the blood contacting surface containing physically adsorbed MPC polymer was shown to be superior in terms of blood compatibility when compared to the same device with a diamond like carbon coating [9,34]. Despite the improved hemocompatibility in these studies, there was con-

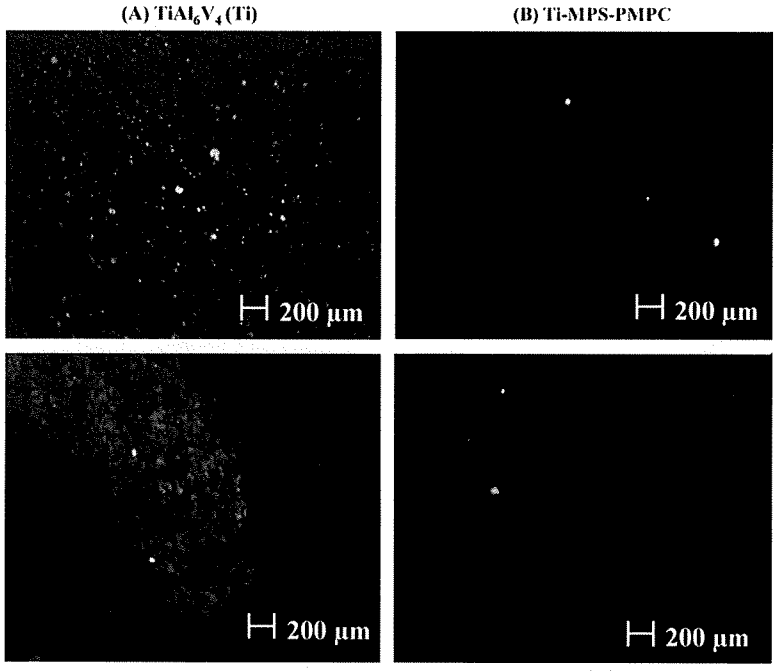

Fig. 4. Fluorescent micrograph images of unmodified and modified $TiAl_6V_4$ samples after contact with minimally anticoagulated (3.0 U/mL heparin) ovine blood for 60 min at 37 °C.

cern about the long term stability of the surface PMPC. Furthermore, in the report of Kihara et al, the physically adsorbed MPC polymer was demonstrated to elute over time during VAD operation [34].

In spite of widespread examination of grafting PC groups onto polymer or silica surfaces, there are few reports where a PC group-bearing polymer has been grafted onto metallic surfaces, and even fewer that have subsequently evaluated the hemocompatibility of the resulting surfaces [36,45,46]. In this study, we showed that a $TiAl_6V_4$ surface could be successfully modified with the MPC moiety by a plasma-induced grafting method after the $TiAl_6V_4$ surface was silanized, and then Ar plasma treated. Our XPS results demonstrated successful modification of the $TiAl_6V_4$ surface with PMPC and the surface showed significant decreases in platelet deposition and activation in comparison with unmodified surfaces. The higher platelet deposition observed on the control Ti–MPS surface relative to the Ti surface could generally be attributed to an increase in surface hydrophobicity as reflected by the higher contact angle of this surface relative to the unmodified Ti alloy. Such an increase in hydrophobicity may serve as a driving force for increased protein adsorption and in this process result in more fibrinogen adsorption in a state that would support platelet adhesion on the surface.

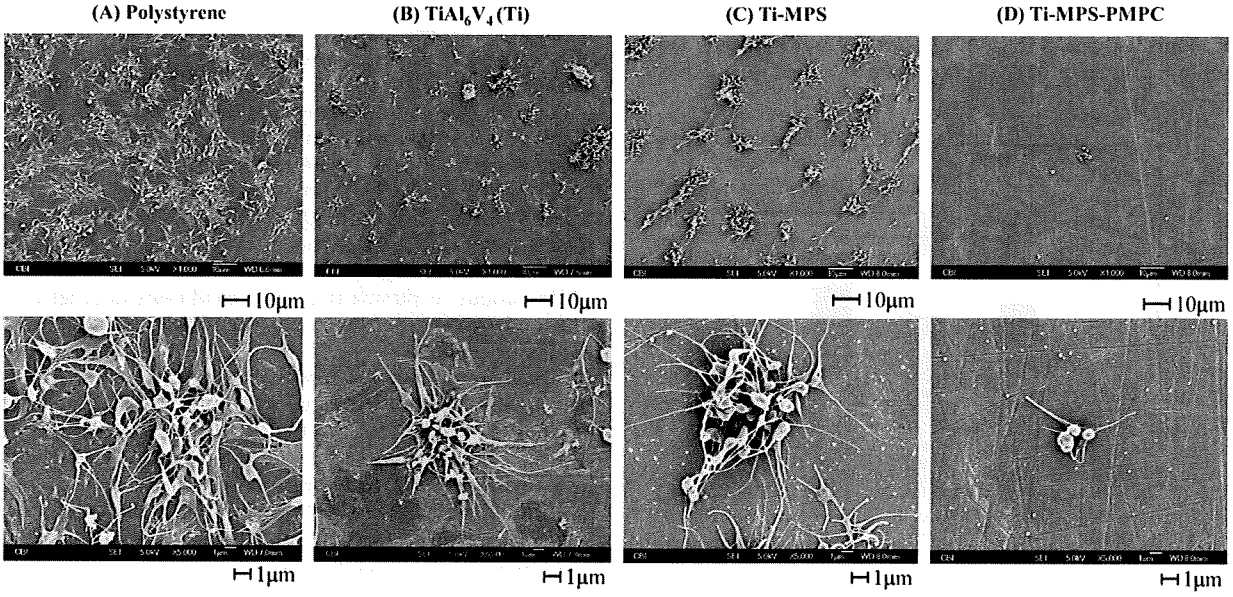

Fig. 5. SEM micrographs of polystyrene, unmodified and modified $TiAl_6V_4$ samples after contact with ovine blood (heparin 6U/mL) for 2.5 h at 37 °C. (A) polystyrene (B) Ti (C) Ti–MPS (D) Ti–MPS–PMPC.

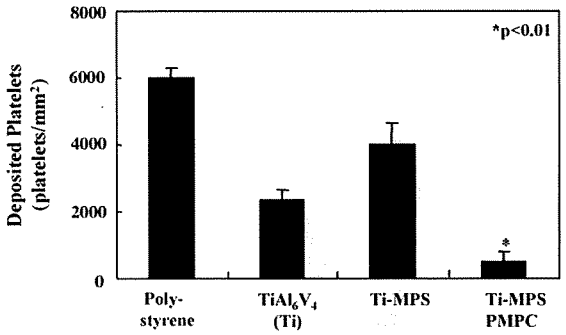

Fig. 6. Platelet deposition onto surfaces after contact with ovine blood for 2.5 h as determined by lactate dehydrogenase (LDH) assay ($n = 3$).

For the PMPC-grafted surface the contact angle and XPS results after a month of mixed water contact were not significantly different from our initial surface tension and XPS evaluation signifying the stability of the grafted PMPC and its sustained hydrophilicity. We previously reported on reduced thrombogenicity after immobilizing an MPC polymer poly(MPC-co-methacryl acid) (PMA) onto titanium surfaces. This surface modification strategy involved a condensation reaction between the carboxyl groups of the PMA and amino groups which were introduced on the titanium surface by a silane coupling agent [34]. However despite its covalent attachment, the long term stability of the PMA immobilized surface is a concern. The cause for concern is that over time the amide bonds between PMA and the titanium surface may be hydrolyzed under continuous blood contact. The PMPC grafting in this report is not linked to the titanium surface via an amide bond, potentially providing an advantage over the PMA immobilized surface in terms of longer-term stability under similar circumstances. Another advantage over the PMA immobilization strategy is that the PMPC grafting technique uses Ar plasma treatment which could be applied to other metallic surfaces, and also on many medically-relevant polymeric surfaces including polytetrafluoroethylene (PTFE).

The PMPC grafting method of this report might allow for more control of PMPC surface coverage and offer improved uniformity of surface PC groups when compared with the previous PMA immobilization method [34]. Immobilization of the long-chain PMA copolymer onto the titanium surface might have caused steric hindrance to further copolymer addition and this may have led to low and non-uniform areas of PMA coverage on the surface. Since the

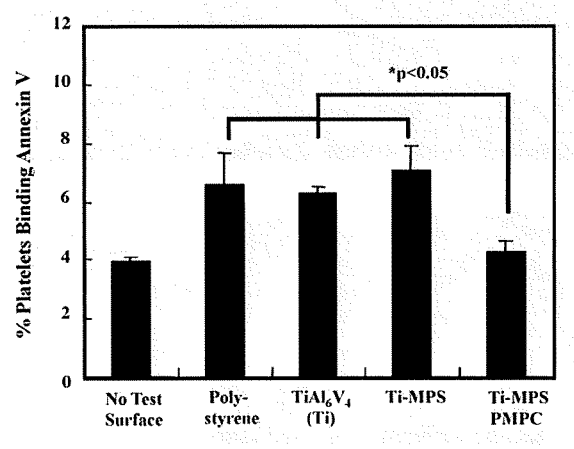

Fig. 7. Quantification of activated platelets in the bulk phase of ovine blood after surface contact under continuous rocking. No test surface indicates blood from a rocked tube into which no test surface was placed. Platelet activation was quantified by flow cytometric measurement of Annexin V binding onto platelets ($n = 3$).

PMPC grafting method employs the addition of MPC rather than the long chain PMA copolymer there is less concern about steric hindrance. Less steric hindrance might lead to higher coverage of the MPC unit on the modified surface provided the surface has sufficient radical formation sites. However it is worth noting that in this grafting method it may be difficult to prepare a surface with 100% MPC unit coverage. This method also has some limitation in terms of the level of control achievable with respect to chain length of the modified PMPC. To obtain better control of the PMPC chain length on the surface, an alternative surface modification method such as surface initiated atom transfer radical polymerization could be considered. If a method were developed to prepare a covalently attached PMPC chain self assembled monolayer on a $TiAl_6V_4$ surface, it would ensure high coverage and uniformity of the PC group and might be even more advantageous in the manufacture of biocompatible blood contacting device surfaces.

In preliminary studies, we chose MPS as a pre-modification agent since it possesses a double bond in its structure and could provide a radical formation site in UV-initiated graft polymerization of MPC. This approach alone, without a UV catalyst, had minimal success (data not shown), so Ar plasma was employed to modify the Ti–MPS surface with the hypothesis that Ar plasma treatment would provide a greater number of radical formation sites, as well as peroxide, on the surface than with UV irradiation alone [18]. The application of both an Ar plasma pre-treatment followed by UV irradiation in the presence of a catalyst such as benzophenone [30,46] on the Ti–MPS surface might have led to even further surface grafting, however this was not investigated.

The graft modification approach using Ar plasma treatment with the PMPC on $TiAl_6V_4$ described in this study might be improved with additional study into ways to further control the surface coverage of the grafted PMPC polymer and therefore maximize the anti-thrombogenic properties of the surface. Several factors that should be considered to improve the surface modification process include control of the water plasma in the MPS silanization process, treatment time under Ar plasma and RFGD power settings. The latter two factors are important in this modification technique since they affect the amount of peroxide groups that are able to become radical formation sites by the decomposition of the peroxide groups [12]. In this study, the Ar plasma treatment time was set to 20 s under 25 W of plasma power at a pressure of 0.6 Torr. Several other Ar treatment time points were evaluated between 0 and 120 s in our preliminary studies. However, the PMPC grafted samples from the 20 s Ar plasma treatment showed the lowest surface contact angle ($18.2° \pm 4.1$) and were used in our subsequent studies. The amount of peroxide concentration generated on the $TiAl_6V_4$ surfaces after the 20 s Ar plasma treatment was $3.4(\pm 1.6) \times 10^{-8}$ mol/cm^2, which was assessed with the plasma treated titanium samples in this study by a peroxide determination method using a 2,2-diphenyl-1-pricylhydrazyl (DPPH) solution [18,19]. However, further study may be necessary to better understand the relationship between the amount of generated peroxide groups and PMPC grafting rate under various Ar plasma treatment conditions in order to establish the best conditions and maximize PMPC incorporation onto the $TiAl_6V_4$ surface.

The MPS modified surface was prepared under hydrolytic condition which allows the methoxy groups in MPS to change to hydroxyl groups and activates the reaction between TiOH and MPS as well as MPS self interaction, thus producing bulk deposition on the surface. Furthermore, the surface roughness might be increased after PMPC grafting, because, the PMPC grafted layer might not be uniform [46]. However the surface roughness or thickness on the MPS and PMPC grafted surface could not measured. We polished the raw titanium alloy sheet by hand with diamond pastes of 3, 1, 0.25 and 0.1 μm size, thus the roughness of the original titanium surface was of a scale that additional texture added from the surface

modification was not likely to be detectable. We chose to use this surface polishing technique since this is the process used industrially to prepare the titanium alloy surfaces before use in blood pump assembly. The surface roughness of the unmodified $TiAl_6V_4$ sample and bulk layer deposition of MPS may have contributed to deviations observed in the atomic composition (Table 1) and contact angle (Table 2) data on the unmodified and modified surfaces. Further study is necessary to measure the surface roughness and thickness of the grafting layer depending on the reaction conditions with a highly polished $TiAl_6V_4$ sample. Fluorescence microscopy observation after staining the PMPC [46], atomic force microscopy and ellipsometry analysis data could be helpful to measure the thickness and roughness of PMPC grafting layer.

In this study, UV irradiation was used to decompose the generated peroxide group and initiate the graft polymerization of MPC. However, the peroxide decomposition also occurs by heating [12,13] and polymerization of MPC might be carried out at 70 °C without UV irradiation if UV irradiation is not appropriate due to complex device geometry. Another limitation to the study is that the blood biocompatibility tests were performed using an in vitro system with ovine blood and under flow conditions that, though mixed, do not replicate any specific application. A next step might be to apply this modification to the interior surfaces of a rotary VAD and assess platelet deposition onto these surfaces in a mock circulatory loop under appropriately high shear blood flow. Comparison studies with other types of modified surfaces such as poly(ethylene glycol)-based or other types of zwitterionic moieties might be of interest to compare the efficacy of this plasma induced grafting technique.

5. Conclusions

$TiAl_6V_4$ surfaces were successfully modified with PMPC chains by a plasma-induced grafting technique following surface silanization and Ar plasma treatment. The PMPC modified $TiAl_6V_4$ surfaces showed significantly decreased platelet deposition and bulk phase platelet activation in vitro relative to the unmodified Ti samples. This PMPC grafting on $TiAl_6V_4$ surfaces shows promise for further investigation as a means to reduce the thromboembolic risk associated with the blood-contacting surfaces of cardiovascular devices. In the setting of a rotary blood pump design, such a coating may allow reduction in anticoagulation levels. Further pre-clinical evaluation is warranted to investigate this potential.

Acknowledgements

This research was supported by NIH contract # HHSN268200448192C and the NSF Engineering Research Center for Revolutionizing Metallic Biomaterials (Award Number: 0812348). Mr. Johnson was supported by a United Negro College Fund MERCK Graduate Science Research Dissertation Fellowship. Mr. Woolley was supported by an NIH training grant # T32-HL076124.

References

[1] H.S. Borovetz, S. Badylak, J.R. Boston, C. Johnson, R. Kormos, M.V. Kameneva, M. Simaan, T.A. Snyder, H. Tsukui, W.R. Wagner, J. Woolley, J. Antaki, C. Diao, S. Vandenberghe, B. Keller, V. Morell, P. Wearden, S. Webber, J. Gardiner, C.M. Li, D. Paden, B. Paden, S. Snyder, J. Wu, G. Bearnson, J.A. Hawkins, G. Jacobs, J. Kirk, P. Khanwilkar, P.C. Kouretas, J. Long, R.E. Shaddy, Cell Transplant. 15 (Suppl. 1 Review) (2006) 69.
[2] D.C. Sin, H.L. Kei, X. Miao, Expert Review of Medical Devices 6 (2009) 51.
[3] W.R. Wagner, H.S. Borovetz, B.P. Griffith, Implantable Cardiac Assist Devices, in: B. Ratner, A. Hoffman, F. Schoen, J. Lemons (Eds.), Biomaterials Science: An Introduction to Materials in Medicine, Elsevier Academic Press, San Diego, CA, 2004, p. 494.
[4] L.R. McBride, K.S. Naunheim, A.C. Fiore, D.A. Moroney, M.T. Swartz, Ann. Thora. Surg. 67 (1999) 1233.
[5] T.A. Snyder, M.J. Watach, K.N. Litwak, W.R. Wagner, Ann. Thorac. Surg. 73 (2002) 1933.
[6] O.H. Frazier, T.J. Myers, I.D. Gregoric, T. Khan, R. Delgado, M. Croitoru, K. Miller, R. Jarvik, S. Westaby, Circulation 105 (2002) 2855.
[7] D.J. Goldstein, Circulation 108 (II) (2003) 272.
[8] A.A. Pitsis, A.N. Visouli, V. Vassilikos, V.N. Ninios, P.D. Sfirakis, N.E. Mezilis, P.S. Dardas, G.S. Filippatos, G.I. Bougioukas, D.T. Kremastinos, J.W. Long, Hellenic J. Cardiol. 47 (2006) 368.
[9] T.A. Snyder, H. Tsukui, S. Kihara, T. Akimoto, K.N. Litwak, M.V. Kameneva, K. Yamazaki, W.R. Wagner, J. Biomed. Mater. Res. 81A (2007) 85.
[10] X. Liu, P.K. Chu, C. Ding, Mater. Sci. Eng. R 47 (2004) 49.
[11] M.C. Deng, L.B. Edwards, M.I. Hertz, A.W. Rowe, B.M. Keck, R.L. Kormos, D.C. Naftel, J.K. Kirklin, D.O. Taylor, Third annual report 2005, J. Heart Lung Transplant. 24 (2005) 1182.
[12] J. Jahanyar, G.P. Noon, M.M. Koerner, K.A. Youker, S.C. Malaisrie, U.Q. Ngo, G.T. Amione, M. Loebe, J. Heart Lung Transplant. 26 (2007) 200.
[13] P.K. Chu, J.Y. Chen, L.P. Wang, N. Huang, Mater. Sci. Eng. R 36 (2002) 143.
[14] E.T. Kang, K.L. Tan, K. Kato, Y. Uyama, Y. Ikada, Macromolecules 29 (1996) 6872.
[15] S.J. Xiao, M. Textor, N.D. Spencer, Langmuir 14 (1998) 5507.
[16] Z.J. Yu, E.T. Kang, K.G. Neoh, K.L. Tan, Surf. Coat. Technol. 138 (2001) 48.
[17] P. Chevallier, M. Castonguay, S. Turgeon, N. Dubrulle, D. Mantovani, P.H. McBreen, J.C. Wittmann, G. Laroche, J. Phys. Chem. B 105 (2001) 12490.
[18] M. Suzuki, A. Kishida, H. Iwata, Y. Ikata, Macromolecules 19 (1986) 1804.
[19] C.Y. Huang, W.L. Lu, Y.C. Feng, Surface Surf. Coat. Technol. 167 (2003) 1.
[20] F. Zhang, E.T. Kang, K.G. Neoh, P. Wang, K.L. Tan, Biomaterials 22 (2001) 1541.
[21] X.P. Zou, E.T. Kang, K.G. Neoh, Surf. Coat. Technol. 149 (2002) 119.
[22] X.P. Zou, E.T. Kang, K.G. Neoh, Plasmas Polym. 7 (2002) 151.
[23] K. Ishihara, Trend Polym. Sci. 5 (1997) 401.
[24] K. Ishihara, T. Ueda, N. Nakabayashi, Polym. J. 22 (1990) 355.
[25] K. Ishihara, H. Nomura, T. Mihara, K. Kurita, Y. Iwasaki, N. Nakabayashi, J. Biomed. Mater. Res. 39 (1998) 323.
[26] A.L. Lewis, Colloids Surf. B: Biointerfaces 18 (2000) 261.
[27] T. Yoneyama, K. Sugihara, K. Ishihara, Y. Iwasaki, N. Nakabayashi, Biomaterials 23 (2002) 1455.
[28] S.H. Ye, J. Watanabe, Y. Iwasaki, K. Ishihara, J. Membr. Sci. 249 (2005) 133.
[29] S.H. Ye, J. Watanabe, Y. Iwasaki, M. Takai, K. Ishihara, Biomaterials 27 (2006) 1955.
[30] T. Goda, T. Konno, M. Takai, T. Moro, K. Ishihara, Biomaterials 27 (2006) 5151.
[31] Y. Hong, S.H. Ye, A. Nieponice, L. Soletti, D.A. Vorp, W.R. Wagner, Biomaterials 30 (2009) 2457.
[32] D.M. Whelan, W.J. Giessen, S.C. Krabbendam, E.A. Vliet, P.D. Verdouw, P.W. Serruys, H.M.M. Beusekom, Heart 83 (2000) 338.
[33] M. Galli, L. Sommariva, F. Prati, S. Zerboni, A. Politi, R. Bonattie, S. Mameli, E. Butti, A. Pagano, G. Ferrari, Catheter Cardiovasc. Interv. 53 (2001) 182.
[34] S. Kihara, K. Yamazaki, P. Litwak, M.V. Kameneva, H. Ushiyama, T. Tokuno, D.C. Borzelleca, M. Umezu, J. Tomioka, O. Tagusari, T. Akimoto, H. Koyanagi, H. Kurosawa, R.L. Kormos, B.P. Griffith, Artif. Organs 27 (2003) 188.
[35] J. Choi, T. Konno, R. Matsuno, M. Takai, K. Ishihara, Colloids Surf. B: Biointerfaces 67 (2008) 216.
[36] S.H. Ye, C.A. Johnson Jr, W.R. Woolley, T.A. Snyder, L.J. Gamble, W.R. Wagner, J. Biomed, Mater. Res. A. 2008, August 5, doi:10.1002/jbm.a.32184.
[37] Y. Tamada, E.A. Kulik, Y. Ikada, Biomaterials 16 (1995) 259.
[38] C.A. Johnson Jr., T.A. Snyder, J.R. Woolley, W.R. Wagner, Artif. Organs 32 (2) (2008) 136.
[39] L.O. Thompson, M. Loebe, G.P. Noon, ASAIO J. 49 (2003) 518.
[40] M. Reynolds, R.M. Delgado III, Curr. Opin. Cardiol. 18 (2003) 199.
[41] T. Mussivand, Artif. Organs 32 (1) (2008) 1.
[42] R.E. Holmlin, X. Chen, R.G. Chapman, S. Takayama, G.M. Whitesides, Langmuir 17 (2001) 2841.
[43] V.A. Tegoulia, W. Rao, A.T. Kalambur, J.F. Rabolt, S.L. Cooper, Langmuir 17 (2001) 4396.
[44] Y.C. Chung, Y.H. Chiu, Y.W. Wu, Y.T. Tao, Biomaterials 26 (2005) 2313.
[45] Y. Iwasaki, N. Saito, Colloids Surf. B: Biointerfaces 32 (2003) 77.
[46] M. Kyomoto, Y. Iwasaki, T. Moro, T. Konno, F. Miyaji, H. Kawaguchi, Y. Takatori, K. Nakamura, K. Ishihara, Biomaterials 28 (2007) 3121.

Colloids and Surfaces B: Biointerfaces 74 (2009) 350–357

Contents lists available at ScienceDirect

Colloids and Surfaces B: Biointerfaces

journal homepage: www.elsevier.com/locate/colsurfb

Nanoscale evaluation of lubricity on well-defined polymer brush surfaces using QCM-D and AFM

Kazuhiko Kitano[a], Yuuki Inoue[b,d], Ryosuke Matsuno[b,c], Madoka Takai[b,c], Kazuhiko Ishihara[a,b,c,d,*]

[a] Department of Bioengineering, The University of Tokyo, 7-3-1, Hongo, Bunkyo-ku, Tokyo 113-8656, Japan
[b] Department of Materials Engineering, School of Engineering, The University of Tokyo, 7-3-1, Hongo, Bunkyo-ku, Tokyo 113-8656, Japan
[c] Center for NanoBio Integration, The University of Tokyo, 7-3-1, Hongo, Bunkyo-ku, Tokyo 113-8656, Japan
[d] Core Research for Evolutional Science and Technology (CREST), Japan Science and Technology Agency, 4-1-8, Honmachi, Kawaguchi, Saitama 332-0012, Japan

ARTICLE INFO

Article history:
Received 17 June 2009
Accepted 6 August 2009
Available online 12 August 2009

Keywords:
2-Methacryloyloxyethyl phosphorylcholine
Polymer brush
Nanoscale interfacial friction force
Quartz crystal microbalance with dissipation
Atomic force microscopy
Nanostructure

ABSTRACT

For preparing a "highly lubricated biointerface", which has both excellent lubricity and biocompatibility, we investigated the factors responsible for resistance to friction during polymer grafting. We prepared poly(2-methacryloyloxyethyl phosphorylcholine) (PMPC), poly(2-hydroxyethyl methacrylate) (PHEMA), and poly(methyl methacrylate) (PMMA) brush layers with high graft density and well-controlled thickness using atom transfer radical polymerization (ATRP). We measured the water absorptivity in the polymer brush layers and the viscoelasticity of the polymer-hydrated layers using a quartz crystal microbalance with dissipation monitoring (QCM-D) measurements. The PMPC brush layer had the highest water absorptivity, while the PMPC-hydrated layer had the highest fluidity. The friction properties of the polymer brush layers were determined in air, water, and toluene by atomic force microscopy (AFM). The friction on each polymer brush decreased only when a good solvent was chosen for each polymer. In conclusion, the brush layer possessing high water absorptivity and fluidity in water contributes to reduce friction. PMPC grafting is an effective and promising method for obtaining highly lubricated biointerfaces.

1. Introduction

In recent years, there has been increasing interest for the surface modification of biomaterials in order to improve their surface properties. All biomaterial surfaces require the ability to suppress biological reactions when they are in contact with living organisms, and we call such contact surfaces as "biointerfaces". Lubricity is also essential for biomaterials such as artificial joints, blood pump bearings, endoscope surfaces, and catheters. The loosening of artificial joints caused by wear between the articulating surfaces is the most serious problem that limits their life and clinical success [1–3]. Biomimetic molecular design of materials is one of the promising approaches to prepare biointerfaces. The cell membrane inspired surface based on phosphorylcholine-group-bearing polymers has shown an excellent resistance to protein adsorption and cell adhesion [4–13]. And also they showed prevention of cell response when they were implanted into tissues. These polymers include 2-methacryloyloxyethyl phosphorylcholine (MPC) units [14]. Poly(MPC) (PMPC) has the ability to resist protein adsorption and also stabilizes functional proteins such as enzymes and antibodies, even when the proteins are immobilized artificially on the surface [15,16]. PMPC is also expected to improve the lubricity of material surfaces since the same phospholipid polar groups are present on the surface of the human articular cartilage. In fact, it has been reported that PMPC grafting onto the polyethylene liner of an artificial hip joint clearly reduces the wear between the articulating surfaces occurring in the long run [17,18]. In this manner, PMPC grafting onto a material surface has already been proved to be an effective method for improving surface lubricity and biocompatibility. PMPC is known to possess a high free water fraction around the chain, which is one of the factors responsible for reducing protein adsorption [15,19]. In this study, we focused on the hydration of grafted polymers and carried out an in-depth investigation of the factors providing both lubricity and biocompatibility on a nanoscale.

We prepared high-density polymer brush layers on a silicon (Si) wafer. Recently, living polymerization techniques have been extensively investigated in order to grow high-density polymer brushes with a controlled length and narrow molecular weight distribution. Atom transfer radical polymerization (ATRP) is one of the best surface-initiated living radical polymerization methods because of its versatility in the choice of monomer types, tolerance to impurities, and mild reaction conditions [20,21]. In this research, we prepared nanoscaled PMPC, poly(2-hydroxyethyl methacrylate)

* Corresponding author at: Center for NanoBio Integration, The University of Tokyo, 7-3-1, Hongo, Bunkyo-ku, Tokyo 113-8656, Japan. Tel.: +81 3 5841 7124; fax: +81 3 5841 8647.
E-mail address: ishihara@mpc.t.u-tokyo.ac.jp (K. Ishihara).

0927-7765/$ – see front matter © 2009 Elsevier B.V. All rights reserved.
doi:10.1016/j.colsurfb.2009.08.004

(PHEMA), and poly(methyl methacrylate) (PMMA) brush layers by ATRP. We investigated the effects of the hydration of the polymer brush layers on resistance to friction on a nanoscale using a quartz crystal microbalance with dissipation monitoring (QCM-D) and an atomic force microscope (AFM). QCM-D allows the simultaneous measurements of mass and viscoelasticity on a material surface through changes in the frequency (F) and energy dissipation (D) in a noninvasive manner. The sensitivity of measurements in the ng/cm^2 range in liquid phase enables us to clarify the dynamic behavior of the polymer brush layer on a nanoscale [22,23]. Using the QCM-D technique, we evaluated the water absorptivity in the polymer brush layers and the viscoelasticity of the polymer-hydrated layers in water. Subsequently, many AFM or lateral force microscope (LFM) studies have been devoted to the understanding of the influence of thin film structure on friction [24–28]. By evaluating the combined results of the QCM-D and AFM measurements, we identified the key factors responsible for obtaining a highly lubricated biointerface.

2. Experimental section

2.1. Materials

MPC was synthesized and purified by the previously reported method [14]. The Si wafers were purchased from Matsushita Electric Industrial Co. (Osaka, Japan). The surfaces of the Si wafers were covered with approximately 100-nm-thick SiO_2 layers. HEMA and MMA were purchased from Kanto Chemical Co. (Tokyo, Japan) and used as received. Copper (I) bromide (CuBr), 2,2′-dipyridyl, and ethyl-2-bromoisobutyrate were purchased from Sigma–Aldrich Co. (St. Louis, USA) and used as received. All the other reagents and solvents were commercially available in extra-pure grade and were used as purchased. Oxygen and argon gases used were of high-purity grade.

2.2. Preparation of the polymer brush layers on the Si wafers

The SiO_2-coated Si wafers were cut into 1.0 cm × 2.0 cm chips, rinsed sufficiently with ethanol and acetone, and etched by oxygen plasma for 20 min (300 W, 100 mL/min gas flow, PR500, Yamato Scientific Co. Ltd., Tokyo, Japan). We used a monochlorosilane, 3-(2-bromoisobutyryl)propyl dimethylchlorosilane (BDCS) as the surface initiator for obtaining a homogeneous monolayer of the initiator on the Si wafers. We synthesized BDCS by the previously described method [29]. The cleaned substrates were immersed in a 5 mmol/L toluene solution of BDCS for 24 h. The wafers were removed from the solution, rinsed with methanol, and dried in an argon stream before being used for graft polymerization. The graft polymerization of MPC, HEMA, and MMA on the Si wafers was performed using ATRP. MPC was dissolved in 10 mL of dehydrated methanol, and HEMA and MMA were dissolved in 10 mL of a mixed solvent comprising 4 parts of methanol and 1 part of water. We used dehydrated methanol as the solvent for MPC since it underwent rapid, uncontrolled polymerization in water [30]. Copper (I) bromide (20 mg, 0.135 mmol) and 2,2′-bipyridyl (43 mg, 0.27 mmol) were added to the solutions of MPC, HEMA, and MMA with stirring under argon at room temperature. The molar ratio of the monomer to the free initiator, [Monomer]/[Initiator], was changed in order to change the polymerization degree, by which we controlled the thickness of the polymer brush layers. After the solution was stirred for 30 min under an argon atmosphere, the BDCS-immobilized Si wafers were immersed into the solution, and simultaneously, ethyl-2-bromoisobutyrate (20 μL, 0.135 mmol) was added as the free initiator. The polymerization was carried out at room temperature with stirring under an argon atmosphere. The Si wafers were removed from the polymerization mixture after the desired time period required for the monomer to completely convert into the corresponding polymer. Subsequently, they were placed in a Soxhlet apparatus, extracted with methanol for 20 h, and dried in vacuo at room temperature. The scheme for the preparation of the PMPC, PHEMA, and PMMA brush layers is shown in Fig. 1. The rates of conversion to the free polymer were confirmed by ^{1}H NMR (JEOL JNM-NR30, Tokyo, Japan). We prepared PMPC with polymerization degrees of 20, 40, 50, 60, 80, 100, 150, and 200 (henceforth each sample will be referred to as PMPC20, PMPC50, ..., PMPC200), and PHEMA and PMMA with polymerization degrees of 50, 100, and 150 (PHEMA/PMMA50, PHEMA/PMMA100, PHEMA/PMMA150). The number after abbreviation represents polymerization degree, that is, PMPC20 is PMPC graft chain consisting of 20 monomer units.

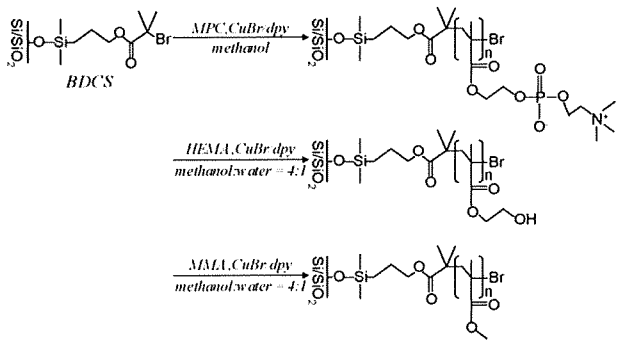

Fig. 1. Synthetic scheme for the fabrication of the PMPC, PHEMA, and PMMA brush layers on a Si wafer surface.

2.3. Surface characterization

The surface elemental composition was determined using X-ray photoelectron spectroscopy (XPS) (AXIS-Hsi, Shimadzu/Kratos, Kyoto, Japan) with a magnesium anode non-monochromatic source. All the samples were completely dried in vacuo before use. High-resolution scans for C_{1s}, O_{1s}, N_{1s}, and P_{2p} were performed at takeoff angles of 90°. All the binding energies were referred to the C_{1s} peak at 285.0 eV. The static water contact angles were measured using a goniometer (CA-W, Kyowa Interface Science Co., Tokyo, Japan) at room temperature. The samples were completely dried in vacuo before the measurements. Water droplets of 6 μL were contacted onto the substrates and the contact angles at 10 s were directly measured by photographic images. The data were collected at three positions on each sample. The thickness of the PMPC, PHEMA and PMMA brush layers on the Si wafers under dry conditions was determined by ellipsometry (DVA-36L3, Mizojiri Optical Co., Tokyo, Japan). Irradiation with a He–Ne laser (632.8 nm) was performed at an incident angle of 70°. The refractive indices (n_r) of Si, PMPC, PHEMA, and PMMA were applied 1.623, 1.488, 1.500, and 1.500, and the extinction coefficients (k_e) were 1.604, 0.000, 0.000, and 0.000, respectively [31]. All the measurements were recorded in air at room temperature. The data were collected at nine locations for each sample. The surface morphologies of the PMPC, PHEMA, and PMMA brush layers were observed with a Nanoscope IIIa AFM (Nihon Veeco, Tokyo, Japan) operated in tapping mode. The measurements were performed under ambient conditions using a standard cantilever at a scan rate of 1.0 Hz. Immediately prior to the measurements, the samples were rinsed by sonication in ethanol and dried in an air stream. The root-mean-square (RMS) surface roughness was calculated from the roughness profiles.

2.4. Measurements of the amount of hydration water and the viscoelasticity of the polymer-hydrated layers

QCM-D is a technique used for measuring the mass of the material/molecules attached to the surface of the quartz crystal via changes in the resonant frequency, ΔF, while simultaneously obtaining information about the viscoelasticity of the layer by measuring the energy dissipation factor, D. The F-shift of the QCM-D is due to the change in the total coupled mass, including that of the water coupled to the layer. In aqueous solvents, the adsorbed film may contain a considerably large amount of water, which is sensed as a mass uptake by the QCM. By measuring the energy dissipation, it becomes possible to judge if the adsorbed film is rigid or elastic which is not possible by merely observing the frequency response. The measurements of F and D were performed with a commercial QCM-D (Q-Sense, Gothenburg, Sweden). The sensor crystals used in the measurements were 5-MHz AT-cut sputter-coated SiO_2 crystals (Q-Sense, Gothenburg, Sweden). The PMPC, PHEMA, and PMMA brush layers were prepared on the sensor crystals via the same ATRP method; [Monomer]/[Initiator] was 100/1 for all the samples. All the measurements were recorded at four different resonant frequencies (5, 15, 25, and 35 MHz). The temperature in the QCM-D liquid chamber was stabilized to 24.5 °C. Q-Sense software was used to acquire the experimental data. We measured the resonant frequencies and dissipation of both the unmodified sensor and the polymer-grafted sensor in air and water. The frequency difference measured between the unmodified sensor and the polymer-grafted sensor in air was defined as ΔF_{air}, and that in water was defined as ΔF_{water}. In a similar manner, the dissipation difference measured between the unmodified sensor and the polymer-grafted sensor in air was defined as ΔD_{air}, and that in water was defined as ΔD_{water}. $\Delta F_{water}/\Delta F_{air}$ is the hydration water ratio, which indicates the mass change due to presence of the hydration water. $\Delta D_{water}/\Delta D_{air}$ is the energy dissipation ratio, which indicates the viscoelastic change due to the hydration. The viscoelasticity of a polymer brush layer includes both the mobility of the polymer chain and fluidity of the hydration water layer.

2.5. Interfacial friction measurements

A Nanoscope IIIa AFM was used to measure the friction force. The experiments were performed in contact mode in air, water, and toluene with several times. Commercially available 200-μm-long V-shaped Si_3N_4 cantilevers (NP-S, Veeco NanoProbe Tips) with an announced force contact of 0.12 N/m were used. The surface friction force data were acquired by scanning in the Trace (T) and Retrace (R) directions with the slow scan axis disabled. The Trace/Retrace pair of scan lines provided a friction loop, and one-half of the separation between the trace and retrace frictions (TMR) was a measure of the friction force. The length of a scan was maintained at 2.0 μm and the scan rate at 2.0 Hz, yielding a sliding velocity of 8.0 μm/s. The applied load N [nN] was varied by changing the vertical deflection of the cantilever. The friction coefficient μ was calculated using Amontons' law ($F = \mu N$).

We converted the experimental normal (V_N) and lateral (V_L) deflection signals expressed in terms of voltage into normal (F_N) and lateral (F_L) forces in Newton by

$$F_N = K_N S_N V_N$$
$$F_L = K_L S_L V_L$$

where K_N and K_L are the normal and lateral force constants [N/m]; and S_N and S_L, the normal and lateral force optical deflection sensitivities [nm/V]. The abovementioned force contact of 0.12 N/m was used as the normal force contact K_N. The lateral force contact K_L was calculated by [32]

$$K_L = \frac{2K_N l^2}{3h^2(1+\upsilon)}$$

where l is the cantilever length [m]; h, the cantilever height [m]; and υ, Poisson's ratio. The S_N values can be obtained from the f–d curve in AFM; S_L is related to S_N by a relation proposed by Liu and Evans [33]. Using these factors, we could convert the voltage signals obtained from AFM into force values. The applied load was also required to be calculated. The applied load N exerted by the cantilever can be given by [34]

$$N = (D - N_0)S_N K_N$$

where D is the value of the deflection setpoint [V]; and N_0, the value of the deflection signal [V] when the cantilever is in its free state. N_0 was determined by the f–d curve measurements (Fig. 2). To obtain the values of S_N and N_0, we measured the f–d curve immediately after every friction force measurement in order to exclude the possible errors induced by the systematic drift.

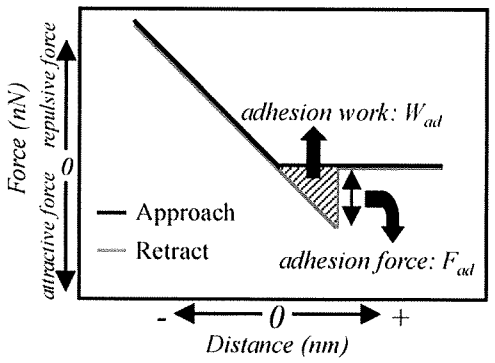

Fig. 2. Schematic illustration of the representative force–distance (f–d) curve measured by AFM and the method for defining F_{ad} and W_{ad}.

3. Results and discussion

3.1. Synthesis of the polymer brush layers via ATRP

We prepared well-controlled PMPC, PHEMA, and PMMA brush layers using ATRP. In order to control the thickness of the polymer graft layers, we controlled the polymerization degree by changing [Monomer]/[Initiator]. From ^{1}H NMR spectrum of the free polymer polymerized in an aqueous medium, we confirmed that the monomer completely converted to the desired polymer under the given conditions.

3.2. Surface characterization

The grafting of PMPC, PHEMA, and PMMA on Si wafers was confirmed using XPS (Fig. 3). The peaks in the carbon atom region (C_{1s}) at 286.5 and 289.0 eV in all the samples indicated the ether bond and ester bond in the methacrylate group, respectively. In the PMPC-grafted substrates, peaks in the nitrogen atom region (N_{1s}) at 403.0 eV attributed to the ammonium group and those in the phosphorus atom region (P_{2p}) at 133.0 eV attributed to the phosphate group were detected. These peaks were specific to the phosphorylcholine group in the PMPC unit.

The relationships of the static water contact angle and the dry thickness with [Monomer]/[Initiator] are shown in Fig. 4. The data in Fig. 4 were measured with high reproducibility and had little difference among the measured positions. The static water contact angles on the PMPC-grafted surfaces ranged from 10° to

25°. The PMPC grafting considerably increased the hydrophilicity, and a slight introduction of the PMPC chains enhanced the wettability. The contact angles on the PHEMA-grafted surfaces were approximately 40°. The hydrophilicity of the PHEMA-grafted surface was also increased. On the other hand, the contact angles on the PMMA-grafted surface were approximately 60°, similar to those on the unmodified Si. The PMMA-grafted surfaces were as hydrophobic as the unmodified Si. The thicknesses of the PMPC, PHEMA, and PMMA brush layers were 4–10, 2–7, and 2–5 nm, respectively. The thicknesses of all the polymer brushes increased with [Monomer]/[Initiator]. We prepared nanostructured polymer brush layers and controlled their thickness by changing the molar ratio of the monomer to the free initiator in the polymerization solution. The graft density σ was calculated using the dry thickness of each polymer brush layer from the equation

$$\sigma = \frac{h\rho N_A}{M_n}$$

where h is the layer thickness [nm] determined by ellipsometry; ρ, the density of each dry polymer layer (1.30 g/cm^3 for PMPC [35], 1.15 g/cm^3 for PHEMA [36], and 1.20 g/cm^3 for PMMA [37]); N_A, Avogadro's number; and M_n, the number-average molecular weight of the polymer chains on the surface. M_n was determined by measuring the molecular weight of the free polymer because these molecular weights had similar values [20]. We calculated M_n from the formula

$$M_n = \mathrm{DP} \times M_0 \times \frac{C}{100}$$

where DP is the polymerization degree determined by [Monomer]/[Initiator]; M_0, the molecular weight of each monomer; and C, the rate of conversion to the polymer determined by ^{1}H NMR measurements. The conversion rate was 100% for all the samples. The graft densities of the PMPC, PHEMA, and PMMA chains were calculated to be 0.17, 0.26, and 0.19 chains/nm^2, respectively. The graft densities of each polymer chain were relatively low compared with those in other literatures [36,37,40]. This would result from the low density of the bromoisobutyryl group at the BDCS-immobilized surface. The BDCS would not be self-assembled at the surface because it has relatively short length of the methylene chains. However, a polymer-grafted layer with a graft density of more than 0.10 chains/nm^2 forms a high-density brush structure [38,39]. It was confirmed that the polymer graft layers prepared via ATRP formed "brush" layers.

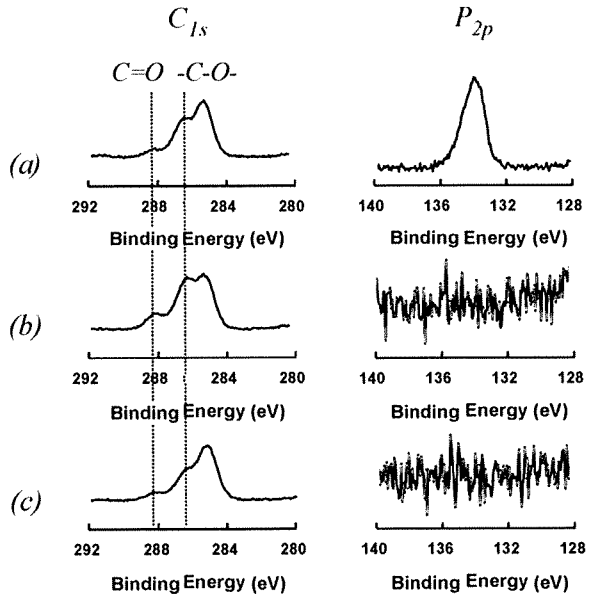

Fig. 3. The XPS spectra of (a) PMPC, (b) PHEMA, and (c) PMMA-grafted surface.

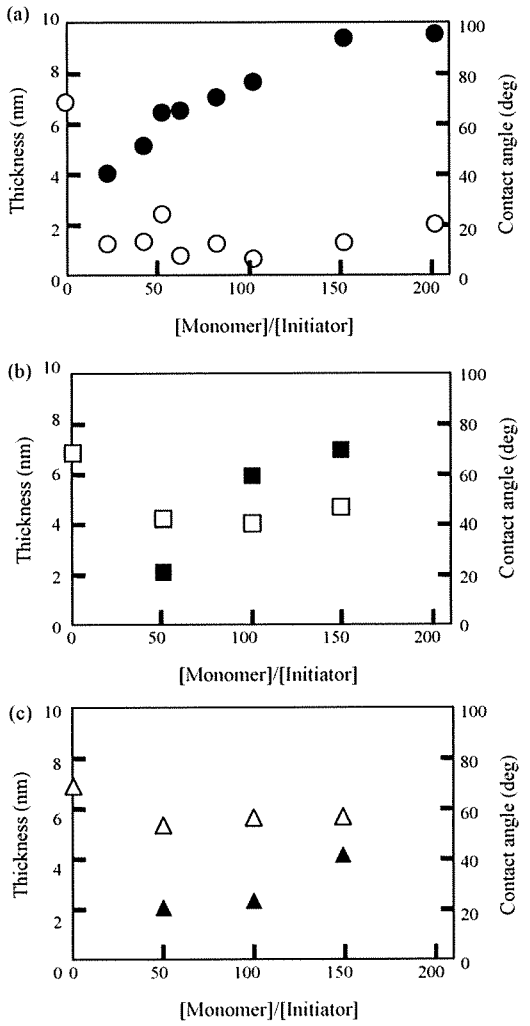

Fig. 4. Relationship between the molar ratio of the monomer to the free initiator and the static water contact angle (open plots) and the thicknesses (closed plots) of (a) the PMPC, (b) PHEMA, and (c) PMMA brush layers.

The brush conformation of the polymer graft layer examined using an AFM in air is shown in Fig. 5. Although the surface of the unmodified Si was nearly flat, the brush-like structure of each polymer graft layer was observed. The RMS surface roughness of all the samples was 0.4–0.8 nm. Compared to previous reports [40], these RMS values were very small, indicating that the polymer brush layers prepared by ATRP were considerably homogeneous with high graft densities.

3.3. Water absorptivity of the polymer brush layers and the viscoelasticity of the polymer-hydrated layers

Fig. 6 shows the hydration water ratio in each polymer brush layer, $\Delta F_{water}/\Delta F_{air}$, and the energy dissipation ratio of each polymer-hydrated layer, $\Delta D_{water}/\Delta D_{air}$. The hydration water ratio for the PMPC brush layer was the highest and decreased in the order PMPC > PHEMA > PMMA. These results indicated that most of the water molecules were coupled to the PMPC brush layer. The results of the hydration water ratio measurements accorded with those

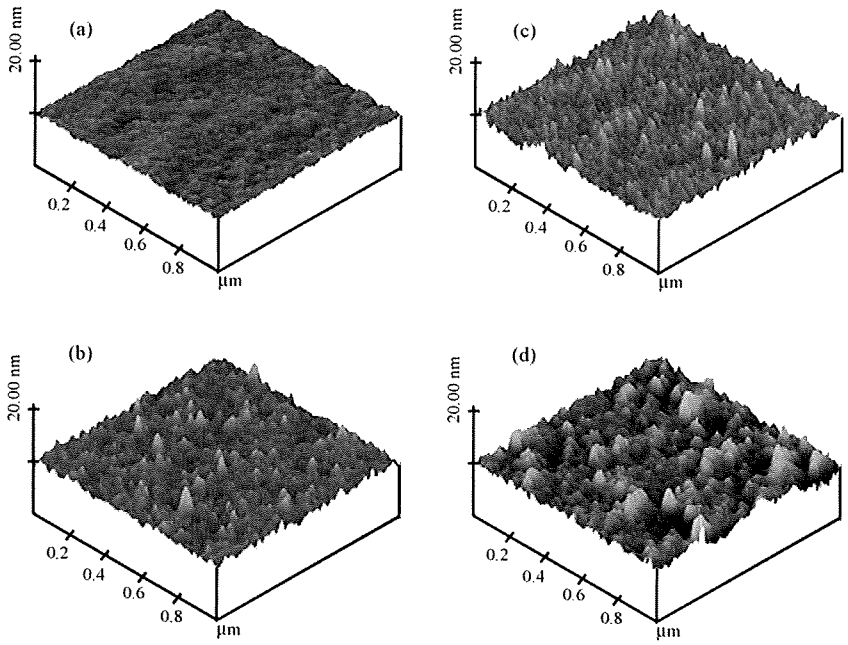

Fig. 5. AFM 3D images of (a) unmodified Si, (b) PMPC100, (c) PHEMA100, and (d) PMMA100 in air.

of the water contact angle measurements. From the values of the energy dissipation ratio, it was apparent that the PMPC-hydrated layer had the maximum fluidity in water; the PHEMA-hydrated layer had the second highest fluidity, while the PMMA-hydrated layer was the most rigid. These results indicate that the hydrophilic PMPC chains and PHEMA chains stretched in water and had greater mobility than the PMMA chains. The $\Delta D_{water}/\Delta D_{air}$ of the PMMA brush layers was negative because the PMMA chains shrink in water and the PMMA-hydrated layer is less fluid than the water layer on the unmodified SiO_2 sensor, whose surface is hydrophilic due to the presence of exposed –OH groups. Moreover, the PMPC-hydrated layer had a high energy dissipation ratio because it possessed a higher free water fraction than that of PHEMA or PMMA [19]. Generally the fluidity of free water is considerably higher than that of binding water. The results of the viscoelasticity measurements of the polymer brush layers well accorded with the previous report on the amount of free water around PMPC, PHEMA, and PMMA [19].

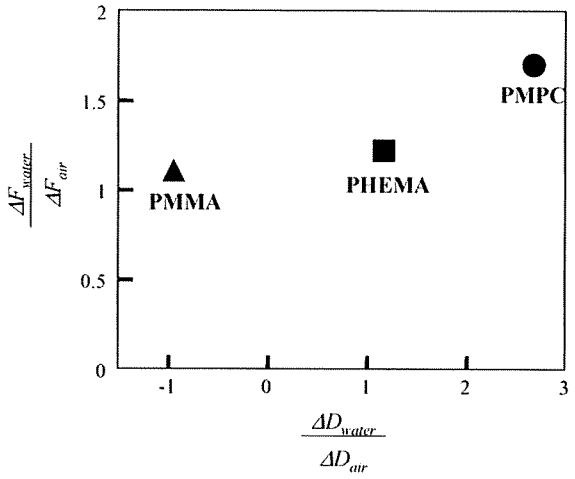

Fig. 6. The hydration water ratio in the polymer brush layer, $\Delta F_{water}/\Delta F_{air}$, and the energy dissipation ratio of the polymer-hydrated layer in water, $\Delta D_{water}/\Delta D_{air}$, measured by QCM-D.

3.4. Friction properties of the polymer brush layers and lubrication mechanism

Kobayashi and Takahara studied the lubrication of PMPC brush surface from viewpoint of macroscopic friction measurements [41]. They observed very low friction on the PMPC brush surface due to high hydrophilicity of the PMPC chains. Very recently, Klein et al. reported the lubrication of PMPC brush surface at physiological pressure and observed extremely low friction coefficient on the surface [42]. This is also due to higher hydration properties of PMPC chains. We investigated the nanoscale interfacial friction forces on the unmodified Si, PMPC, PHEMA, and PMMA brush layers using an AFM in contact mode. The representative values of the friction coefficients calculated as a function of the normal load are shown in Fig. 7. In air (Fig. 7 (a)), the friction coefficients of the PMPC brush layers were the same as those of the unmodified Si, and were characteristically high under a load less than 20 nN. When the load was above 20 nN, the friction coefficients of all the samples in air were stabilized at approximately 0.2. In contrast, in water (Fig. 7 (b)), the friction coefficients of the PMPC brush layers considerably decreased, and were below 0.08 when the load was below 20 nN. Then, the friction coefficients of the PMPC brush layers gradually increased with the normal load, and those of PMPC50, PMPC100, and PMPC150 were stabilized at approximately 0.09, 0.06, and 0.03, respectively. The friction coefficients of the PMPC brush layers in water decreased with an increase in their thicknesses of the PMPC brush layer. Fig. 7 (c) shows the friction coefficient of the PHEMA brush layers in water. When the load was below 20 nN, the friction coefficients of PHEMA50 were above 0.12, while those of PHEMA100 and PHEMA150 were below 0.12. As the normal load increased, the friction coefficients of all the PHEMA brush layers approached to approximately 0.10. Fig. 7 (d) shows the friction coefficients of the PMMA brush layers in water and those of PMMA100 in toluene. The friction coefficients of all the PMMA brush layers in water were high (above 0.2) when the

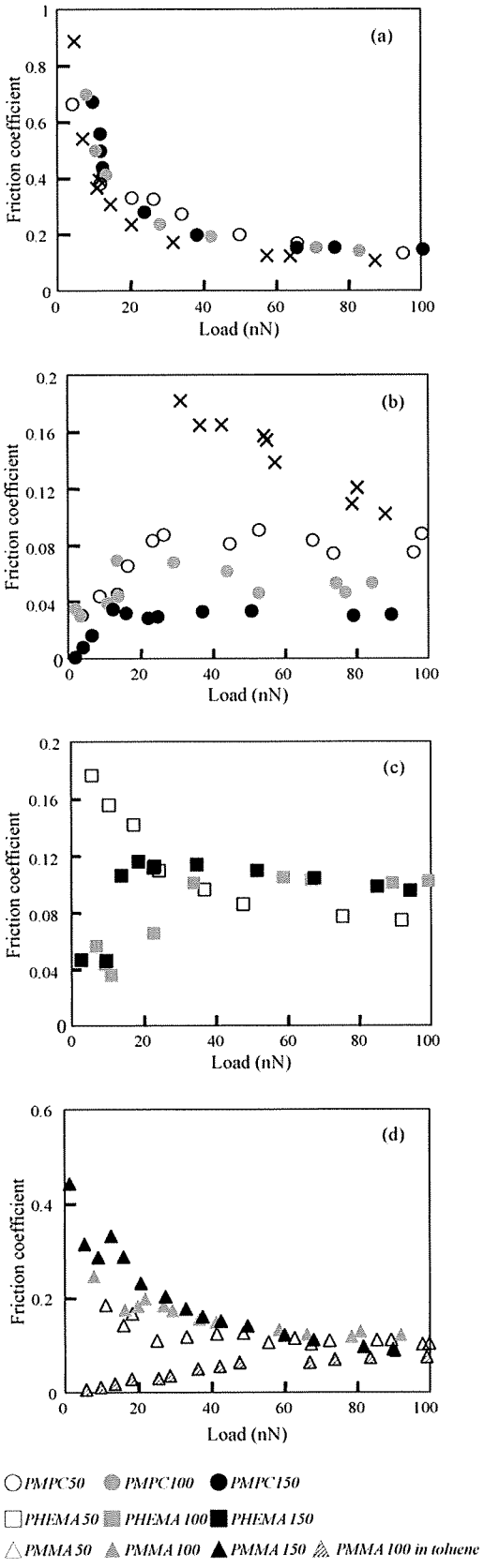

Fig. 7. The friction properties of the polymer brush layers measured by AFM: (a) the friction coefficients of the unmodified Si, PMPC50, PMPC100, and PMPC150 measured in air; (b) the friction coefficients of the unmodified Si, PMPC50, PMPC100, and PMPC150 measured in water; (c) the friction coefficients of the PHEMA50, PHEMA100, and PHEMA150 measured in water; (d) the friction coefficients of the PMMA50, PMMA100, and PMMA150 measured in water and PMMA100 measured in toluene.

load was below 20 nN. Subsequently, these values were gradually stabilized at approximately 0.15. In toluene, however, the friction coefficients of PMMA100 were clearly reduced. The friction coefficients of PMMA100 in toluene were below 0.04 when the load was below 20 nN, and gradually increased with the normal load.

The high friction coefficients for the load below 20 nN in these experiments were due to the adhesion force between the AFM cantilever and the substrate. The adhesion force between the AFM cantilever and the unmodified Si surface was 10–30 nN, as measured by the *f*–*d* curves, and acted as the load. When the load was below 20 nN, the adhesion force significantly influenced the load, thus magnifying the friction coefficients. The same adhesion force was measured on the PMPC brush layers in air. It was considered that the PMPC chains shrunk in air and were unable to prevent the interaction between the AFM cantilever and the substrate. In addition, the PMMA chains shrunk in water, and the AFM cantilever slid on the solid surface because water was a poor solvent for PMMA. The friction of the polymer brush layer only decreased when a good solvent was used for each polymer. No adhesion force between the AFM cantilever and the PMPC and PHEMA brush layers was observed in water, and a similar effect was also detected on the PMMA brush layer in toluene. In a good solvent, the polymer chains stretch and form a solvated layer that prevents the direct contact of the AFM cantilever with the substrate. Satisfying the condition of isolated friction interfaces leads to very low friction. As the normal load increased, the AFM cantilever penetrated the brush layer, and its interaction with the substrate gradually increased.

Correlating these friction properties with the results of the QCM-D measurements, it was found that both the hydration water ratio and energy dissipation ratio of the polymer-hydrated layer in water were strongly related to the friction resistance (Fig. 8). This result is consistent with the general friction theory. A usual friction phenomenon between solid surfaces is explained by the Bowden–Tabor theory [43]. In this theory, real surfaces in contact would only meet at the small areas at the peaks of their inevitable surface roughness, known as adhesion areas, where the pressure would be high and friction would be generated. In this case, friction mainly depends on the shear forces occurring at the adhesion areas, and the friction coefficient calculated by Amontons' law becomes 0.2–1.0. On the other hand, when a gas or liquid layer separates the friction interfaces and the adhesion area is absent, the friction clearly decreases. This condition is termed as hydrodynamic lubrication, and friction force F is given by [43]

$$F = \frac{\eta A v}{D}$$

where η is the viscosity of the gas or liquid layer [Ns/m^2]; A, the contact area [m^2]; v, the sliding velocity [m/s]; and D, the surface separation [m]. If the friction conditions, such as sliding size, sliding velocity, and materials used, are the same, the friction mainly depends on the surface separation distance and viscosity resistance of the layer separating the friction interfaces. The friction coefficient was dependent on the water absorptivity, because high water absorptivity led to the formation of a thick hydrated layer and large surface separation distance. Tsujii et al. have reported that the length of high-density polymer brush chains in a good solvent was approximately 2.5 times as that under dry conditions [38]. Therefore, a thick polymer brush layer could form a thick hydrated layer. This is because the friction coefficients of the PMPC and PHEMA brush layers in water depended on the thickness of

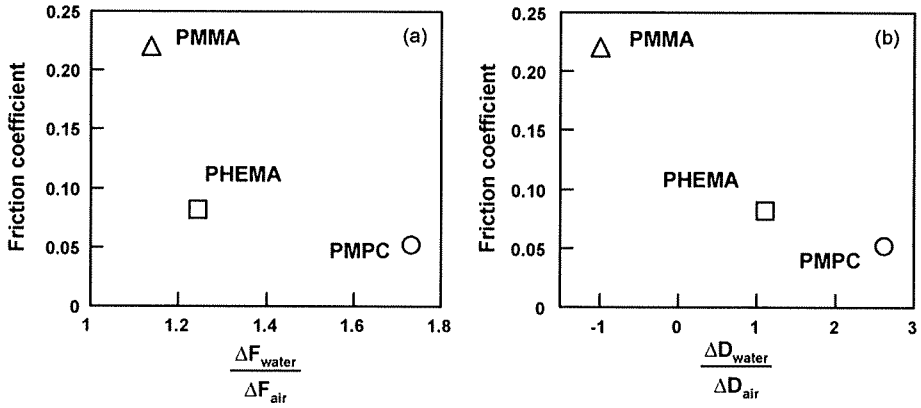

Fig. 8. Relationship (a) between the hydration water ratio, $\Delta F_{water}/\Delta F_{air}$, and the friction coefficient, and (b) between the energy dissipation ratio of the polymer-hydrated layers, $\Delta D_{water}/\Delta D_{air}$, and the friction coefficient.

the brush layers. The grafting method is significant in effecting the surface separation because a polymer layer binds to a substrate through a chemical reaction. Several previous studies have revealed that physically adsorbed polymer chains do not provide adequate wear characteristics because the physisorbed layers are observed to quickly wear away under repeated sliding cycles [44,45]. We also have reported that the polypropylene surface grafted with PMPC via a photoinduced graft polymerization method showed a good resistance against high pressure and repeated sliding cycles [46]. The dissipation ratio of the polymer-hydrated layer was related to the viscosity resistance of the layer. The high fluidity of the PMPC-hydrated layer led to low viscosity resistance. These results accorded with those mentioned in previous reports. Galliano et al. have reported lower friction coefficients for crosslinked polydimethylsiloxane (PDMS) networks with large mesh sizes; they contended that this resulted from the presence of a greater number of free and pendant chains at the interface of the large-mesh-size networks as compared to those in more tightly crosslinked networks possessing smaller mesh sizes [47]. Similar results have been reported by Gong et al. in their study of the interfacial friction of hydrogels [48,49]. They found that gels having brush-like dangling chains on their surface could manifest friction forces that were 1–2 orders of magnitude lower than those of gels without these dangling chains. These two reports indicated that the surface separation was caused by crosslinked PDMS networks or gels, and that the fluidity of the layer was caused by free and pendant chains or brush-like dangling chains.

4. Conclusions

In order to investigate the key factors responsible for the improvement of the lubricity of material surfaces, we prepared three kinds of well-controlled polymer brush layers with different monomer units and characterized them at a nanoordered level using a QCM-D and an AFM. The friction resistance was strongly correlated to the water absorptivity and fluidity of the polymer-hydrated layer. Increasing the surface separation distance with polymer-hydrated layer is the first key factor for obtaining a highly lubricated biointerface, and the high fluidity of the polymer-hydrated layer is the second key factor. PMPC grafting is a very effective and promising method for achieving both the abovementioned factors.

Acknowledgment

We thank Dr. Tomohiro Konno, the University of Tolyo and Dr. Masayuki Kyomoto, Japan Medical Materials, for providing useful discussions. Also, we are indebted to Prof. Takao Hanawa at Tokyo Medical and Dental University for ellipsometry measurements. A part of the research was supported by G-COE program "Center for Medical System Innovation".

References

[1] W.H. Harris, Clin. Orthop. 311 (1995) 46–53.
[2] A. Kobayashi, M.A. Freeman, W. Bonfield, Y. Kadoya, T. Yamac, N. Al-Saffar, G. Scott, P.A. Revell, J. Bone Joint Surg. Br. 79 (1997) 844–848.
[3] D.H. Sochart, Clin. Orthop. 363 (1999) 135–150.
[4] H. Lomas, M. Massignani, K.A. Abdullah, I. Canton, C. Lo Presti, S. MacNeil, J. Du, A. Blanazs, J. Madsen, S.P. Armes, A.L. Lewis, G. Battaglia, Faraday Discuss. 139 (2008) 143–159.
[5] K. Ishihara, M. Takai, J.R. Soc. Interf. 6 (2009) S279–S291.
[6] K. Ishihara, R. Aragaki, T. Ueda, A. Watanabe, N. Nakabayashi, J. Biomed. Mater. Res. 24 (1990) 1069–1077.
[7] K. Ishihara, N.P. Ziats, B.P. Tierney, N. Nakabayashi, J.M. Anderson, J. Biomed. Mater. Res. 25 (1991) 1397–1407.
[8] K. Ishihara, H. Oshida, Y. Endo, T. Ueda, A. Watanabe, N. Nakabayashi, J. Biomed. Mater. Res. 26 (1992) 1543–1552.
[9] S. Sawada, Y. Iwasaki, N. Nakabayashi, K. Ishihara, J. Biomed. Mater. Res. 79 (2006) 476–484.
[10] K. Sugiyama, K. Ohga, H. Aoki, Macromol. Chem. Phys. 196 (1995) 1907–1916.
[11] T. Oishi, H. Uchiyama, K. Onimura, H. Tsutsumi, Polym. J. 30 (1998) 17–22.
[12] L. Ruiz, J.G. Hilborn, D. Leonard, H.J. Mathieu, Biomaterials 19 (1998) 987–998.
[13] Y. Wang, T.J. Su, R. Green, Y. Tang, D. Styrkas, T.N. Danks, R. Bolton, J.R. Lu, Chem. Commun. (2000) 587–588.
[14] K. Ishihara, T. Ueda, N. Nakabayashi, Polym. J. 22 (1990) 355–360.
[15] K. Ishihara, H. Nomura, T. Mihara, K. Kurita, Y. Iwasaki, N. Nakabayashi, J. Biomed. Mater. Res. 39 (1998) 323–330.
[16] W. Feng, S. Zhu, K. Ishihara, J.L. Brash, Biointerphases 1 (2006) 50–60.
[17] T. Moro, Y. Takatori, K. Ishihara, T. Konno, Y. Takigawa, T. Matsushita, U. Chang, K. Nakamura, H. Kawaguchi, Nat. Mater. 3 (2004) 829–836.
[18] M. Kyomoto, T. Moro, T. Konno, H. Takadama, N. Yamasaki, H. Kawaguchi, Y. Takatori, K. Nakamura, K. Ishihara, J. Biomed. Meter. Res. Part A 82 (2007) 10–17.
[19] H. Kitano, M. Imai, T. Mori, M. Gemmei-Ide, Y. Yokoyama, K. Ishihara, Langmuir 19 (2003) 10260–10266.
[20] M. Husseman, E.E. Malmstrom, M. McNamara, M. Mate, D. Mecerreyes, D.G. Benoit, Macromolecules 32 (1999) 1424–1431.
[21] J. Pyun, T. Kowalewski, K. Matyjaszewski, Macromol. Rapid Commun. 24 (2003) 1043–1059.
[22] M.T. Muller, X. Yan, S. Lee, S.S. Perry, N.D. Spencer, Macromolecules 38 (2005) 5706–5713.
[23] A.K. Dutta, G. Belfort, Langmuir 23 (2007) 3088–3094.
[24] R. Kaneko, Tribol. Int. 28 (1995) 195.
[25] B. Bhushan, Proc. Inst. Mech. Eng. Part J 212 (1998) 1.
[26] J. Hu, X. Xiao, D.F. Ogletree, M. Salmeron, Surf. Sci. 327 (1995) 358.
[27] S.W. Zhang, H.Q. Lan, Tribol. Int. 35 (2002) 321.
[28] Q. Zhang, L.A. Archer, Langmuir 23 (2005) 7562–7570.
[29] A. Ramakrishnan, R. Dhamodharan, J. Ruhe, Macromol. Rapid Commun. 23 (2002) 612–616.
[30] I.Y. Ma, J. Lobb, N.C. Billingham, S.P. Armes, A.L. Lewis, A.W. Lloyd, J. Salvage, Macromolecules 35 (2002) 9306–9314.
[31] S. Hu, Y. Wang, K. McGinty, W.J. Brittain, Eur. Polym. J. 42 (2006) 2053–2058.
[32] E. Tocha, H. Schonherr, G.J. Vancso, Langmuir 22 (2006) 2340–2350.
[33] Y. Liu, D.F. Evans, Langmuir 12 (1996) 1235–1244.
[34] J. Li, C. Wang, G. Shang, Q. Xu, Z. Lin, J. Guan, C. Bai, Langmuir 15 (1999) 7662–7669.

[35] R. Iwata, P. Suk-In, V.P. Hoven, A. Takahara, K. Akiyoshi, Y. Iwasaki, Biomacromolecules 5 (2004) 2308–2314.
[36] C. Yoshikawa, A. Goto, Y. Tsujii, T. Fukuda, T. Kimura, K. Yamamoto, A. Kishida, Macromolecules 39 (2006) 2284–2290.
[37] B. Chao, Langmuir 20 (2004) 11748–11755.
[38] Y. Tsujii, K. Ohno, S. Yamamoto, A. Goto, T. Fukuda, Adv. Polym. Sci. 197 (2006) 1–45.
[39] T. Wu, K. Efimenko, J. Genzer, J. Am. Chem. Soc. 124 (2002) 9394–9395.
[40] W. Feng, J.L. Brash, S. Zhu, Biomaterials 27 (2006) 847–855.
[41] M. Kobayashi, Y. Terayama, N. Hosaka, M. Kaido, A. Suzuki, N. Yamada, N. Torikai, K. Ishihara, A. Takahara, Soft Mater. 3 (2007) 740–746.
[42] M. Chen, W.H. Briscoe, S.P. Armes, J. Klein, Science 323 (2009) 1698–1701.
[43] D.F. Moore, Principle and Application of Tribology, Pergamon Press, Oxford, 1975.
[44] V.V. Tsukruk, Adv. Mater. 13 (2001) 95–108.
[45] T. Bouhacina, J.P. Aime, D. Gauthier, V. Michel, V. Heroguez, Phys. Rev. B 56 (1997) 7694–7703.
[46] K. Kitano, R. Matsuno, T. Konno, M. Takai, K. Ishihara, Trans. Mater. Res. Soc. Japan 32 (2007) 579–582.
[47] A. Galliano, S. Bistac, J.J. Schultz, Colloid Interf. Sci. 265 (2003) 372–379.
[48] J.P. Gong, T. Kurokawa, T. Narita, G. Kagata, Y. Osada, G. Nishimura, M. Kinjo, J. Am. Chem. Soc. 123 (2001) 5582–5583.
[49] T. Tada, D. Kaneko, J.P. Gong, T. Kaneko, Y. Osada, Tribol. Lett. 17 (2004) 505–511.

ORIGINAL ARTICLE

Effect of Lubricant on Wear Behavior of Ultrahigh-molecular-weight Polyethylene Cups Against Zirconia Head in Hip Joint Simulator

Masami HASHIMOTO[1], Mineo MIZUNO[1], Satoshi KITAOKA[1], Hiroaki TAKADAMA[2], and Masaru UENO[3]

[1] Japan Fine Ceramics Center, Nagoya, Japan
[2] Chubu University, Nagoya, Japan
[3] Japan Medical Materials Corporation, Osaka, Japan